NeuroImage 224 (2021) 117394

Contents lists available at ScienceDirect

NeuroImage

journal homepage: www.elsevier.com/locate/neuroimage

Transcranial magnetic stimulation and magnetic resonance spectroscopy: Opportunities for a bimodal approach in human neuroscience

Koen Cuypers[a,b], Anouk Marsman[c,*]

[a] Department of Movement Sciences, Group Biomedical Sciences, Movement Control & Neuroplasticity Research Group, KU Leuven, 3001 Heverlee, Belgium
[b] REVAL Research Institute, Hasselt University, Agoralaan, Building A, 3590 Diepenbeek, Belgium
[c] Danish Research Centre for Magnetic Resonance, Centre for Functional and Diagnostic Imaging and Research, Copenhagen University Hospital Hvidovre, Section 714, Kettegård Allé 30, 26500 Hvidovre, Denmark

ARTICLE INFO

Keywords:
Plasticity
Transcranial magnetic stimulation (TMS)
Magnetic resonance spectroscopy (MRS)
Gamma-aminobutyric acid (GABA)
Glutamate
N-acetyl aspartate (NAA)

ABSTRACT

Over the last decade, there has been an increasing number of studies combining transcranial magnetic stimulation (TMS) and magnetic resonance spectroscopy (MRS). MRS provides a manner to non-invasively investigate molecular concentrations in the living brain and thus identify metabolites involved in physiological and pathological processes. Particularly the MRS-detectable metabolites glutamate, the major excitatory neurotransmitter, and gamma-aminobutyric acid (GABA), the major inhibitory neurotransmitter, are of interest when combining TMS and MRS. TMS is a non-invasive brain stimulation technique that can be applied either as a neuromodulation or neurostimulation tool, specifically targeting glutamatergic and GABAergic mechanisms. The combination of TMS and MRS can be used to evaluate alterations in brain metabolite levels following an interventional TMS protocol such as repetitive TMS (rTMS) or paired associative stimulation (PAS). MRS can also be combined with a variety of non-interventional TMS protocols to identify the interplay between brain metabolite levels and measures of excitability or receptor-mediated inhibition and facilitation. In this review, we provide an overview of studies performed in healthy and patient populations combining MRS and TMS, both as a measurement tool and as an intervention. TMS and MRS may reveal complementary and comprehensive information on glutamatergic and GABAergic neurotransmission. Potentially, connectivity changes and dedicated network interactions can be probed using the combined TMS-MRS approach. Considering the ongoing technical developments in both fields, combined studies hold future promise for investigations of brain network interactions and neurotransmission.

1. Introduction

Since their introduction more than 30 years ago, transcranial magnetic stimulation (TMS) and magnetic resonance spectroscopy (MRS) are commonly used for studying the healthy and pathological human brain. Only recently, both techniques are combined for mainly two purposes. On the one hand, studies aimed at evaluating alterations of metabolite levels assessed with MRS following an interventional TMS protocol such as repetitive TMS (rTMS) or paired associative stimulation (PAS). On the other hand, the combination of MRS and a variety of non-interventional TMS protocols was applied to identify the interplay between MRS-based metabolite levels and TMS-based measures of excitability or receptor-mediated inhibition and facilitation in the human motor system. In this review, firstly, TMS and MRS will be introduced, focusing on techniques and measures that are commonly used when combining the two methods. Secondly, an overview of the literature combining both techniques will be provided. Thirdly, limitations will be discussed. And finally, future perspectives and opportunities will be explored.

1.1. TMS

TMS is a non-invasive brain stimulation technique that can be applied either as a neuromodulation or neurostimulation tool (Fig. 1). By holding a TMS coil over the skull, underlying brain tissue can be stimulated when a sufficiently strong stimulus is administered. The mechanism of TMS is based on the principle of electromagnetic induction. Specifically, a magnetic field is produced by an electrical current in the coil. When this magnetic field is rapidly changed, an electrical current is induced in the underlying tissue. Depending on the stimulation parameters and the protocol, TMS can be used for various applications. In the next section, only TMS techniques that are currently combined with MRS are discussed (for a review, see Klomjai et al., 2015; Chen et al., 2008).

* Corresponding author.
E-mail address: anoukm@drcmr.dk (A. Marsman).

https://doi.org/10.1016/j.neuroimage.2020.117394
Received 20 March 2020; Received in revised form 18 August 2020; Accepted 17 September 2020
Available online 26 September 2020

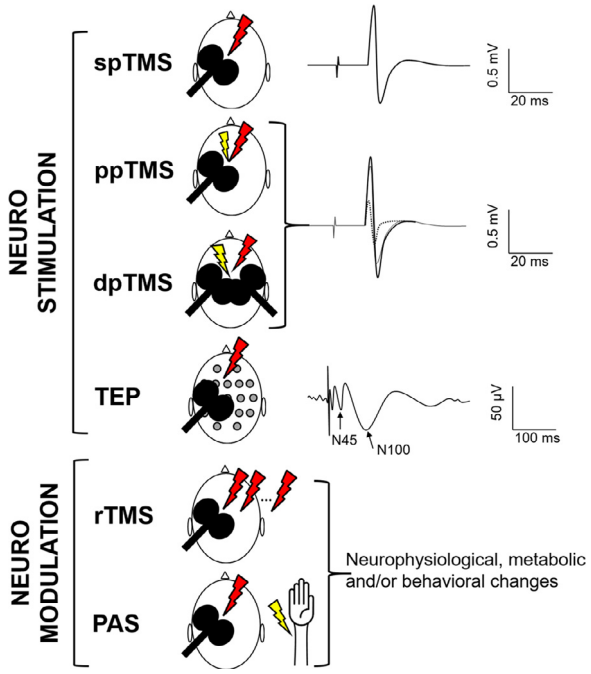

Fig. 1. Overview of the most common TMS techniques used for neurostimulation and neuromodulation and their outcomes when combining TMS with MRS. Neurostimulation protocols include single-pulse TMS (spTMS), paired-pulse TMS (ppTMS), dual-site TMS (dsTMS) and TMS-evoked EEG potentials (TEP). Neuromodulation protocols include repetitive TMS (rTMS) and paired-associative stimulation (PAS). Red arrows indicate regular TMS (or test) pulses and yellow arrows indicate conditioning pulses. For sp-, pp-, and dsTMS outcomes are measures as a motor evoked potential (MEP). For pp- and dsTMS the combination of a conditioning pulse and a test pulse can induce inhibition (red dashed line) of facilitation (green dasched line) as compared to the unconditioned (spTMS) condition (solid black line). For TEP, the N45 and N100 (negative deflection at a latency of 45 and 100 ms) components are often reported as they are linked to respectively, $GABA_A$ and $GABA_A$ or $GABA_B$-mediated inhibition.

1.1.1. *TMS for neuromodulation*

When a train of consecutive pulses is applied, TMS can modulate brain activity, depending on the stimulation frequency. This interventional protocol is referred to as rTMS. Overall, low-frequency rTMS (around 1 Hz) has been observed to mostly result in cortical inhibition (Chen et al., 1997), while facilitatory effects were reported after high-frequency rTMS (5–50 Hz) (Maeda et al., 2000; Pascual-Leone et al., 1994). An rTMS paradigm that has also been shown effective is theta burst stimulation (TBS) (Huang et al., 2005). During TBS, trains consisting of three pulses at a rate of 50 Hz and usually an intensity of 80% of the active motor threshold (aMT; see definition below) are applied and repeated with an intertrain interval (ITI) of 200 ms (5 Hz). When applying a continuous TBS protocol (cTBS, 600 pulses over 40 s), inhibitory aftereffects lasting up to one hour can be achieved, however test-retest reliability of cTBS aftereffects was reported to be low to moderate (Jannati et al., 2019). In contrast to cTBS, intermittent TBS (iTBS, 600 pulses over 190 s consisting if 2 s trains repeated every 10 s) leads to facilitatory aftereffects lasting up to 15 min (Huang et al., 2005).

PAS is another TMS protocol that can induce neuronal excitability changes in the motor cortex (for a review, see Classen et al., 2004). Here, consecutive pairs (typically 90–200) of electrical peripheral nerve stimuli and single TMS pulses at the contralateral motor cortex are administered at low frequency (0.05 Hz). The effect of PAS depends on the interstimulus interval (ISI). Moreover, an ISI of 10 ms results in a depression of excitability, whereas an ISI of 25 ms generates excitability (Wolters et al., 2003). PAS-induced aftereffects can last up to one hour (Stefan et al., 2000).

1.1.2. *TMS for neurostimulation*

1.1.2.1. Corticospinal excitability and central motor conduction time. When applied over the primary motor cortex (M1), single-pulse (sp) TMS and TMS recruitment curves are protocols that reveal outcome measures that relate to corticospinal excitability and which can be quantified by assessing the electromyographical (EMG) output at the target muscle(s). From an spTMS protocol, parameters such as motor evoked potential (MEP) size, motor threshold (MT), central motor conduction time (CMCT) and several other parameters can be derived. MT and MEP size are the most basic TMS measures to assess corticospinal excitability. The MT can be assessed for a muscle in rest (rMT) or during activity (i.e. during isometric voluntary contraction) (aMT). MT is often defined as the stimulator output required to obtain a least 5 out of 10 MEPs above a predefined threshold, for example ≥50 μV (Rossini et al., 1994), and is commonly used to define individualized TMS intensity parameters (Wassermann, 2002). The MEP size, measured as the peak-to-peak amplitude, is assumed to reflect the number of activated corticospinal motor neurons. Due to the variability inherent to TMS and in order to obtain a reliable estimate of corticospinal excitability, it is recommended to measure the average MEP over several consecutive trials (Cuypers et al., 2014). Recruitment curves reflect the input-output characteristics of the corticospinal motor system. With this protocol, a series of single TMS pulses of variable strength (input) is administered in a randomized order over M1 and for each pulse, the corresponding MEP (output) is measured using EMG. Several parameters such as, for example, the slope of the curve, the stimulation intensity required to reach saturation (plateau) and the area under the recruitment curve (AURC) can be extracted from the data. While the slope of the curve and the AURC are considered markers of corticospinal projection strength (Chen et al., 1998; Carson et al., 2013), the stimulation intensity to reach saturation indicates that all targeted neurons are excited (Kukke et al., 2014).

The CMCT is defined as the time it takes for neural impulses to travel through the central nervous system on their way to the target muscles (Udupa and Chen, 2013). This timing is calculated by subtracting the peripheral motor conduction time from the MEP latency. According to Chen et al., 2008, the CMCT includes the times for excitation of cortical cells, conduction via corticospinal (or corticobulbar) tracts and excitation of the motor neuron sufficient to exceed its firing threshold (Chen et al., 2008).

1.1.2.2. TMS-based measures of excitability and receptor-mediated inhibition and facilitation. At the M1, spTMS can be used to measure cortical silent periods (CSP) (Inghilleri et al., 1993; Kujirai et al., 1993), reflecting gamma-aminobutyric acid type A ($GABA_A$) or type B ($GABA_B$) receptor-mediated inhibition (Ziemann et al., 2015). It is suggested that later parts of CSPs reflect $GABA_B$ receptor-mediated inhibition while initial parts of CSPs reflect $GABA_A$ receptor-mediated inhibition. This protocol requires a sustained voluntary isometric contraction of the target muscle while at the same time a single TMS pulse is administered over the contralateral M1. Consequently, a MEP can be elicited in the target muscle followed by the CSP, which refers to the period of decreased EMG signal starting immediately after spTMS administration and ending when EMG activity is restored to baseline (EMG activity during voluntary isometric contraction).

In paired-pulse (pp) TMS protocols, a series of unconditioned (single) and conditioned (paired) pulses are administered to M1. Next, the ratio between the averaged conditioned and unconditioned MEP amplitude is calculated. If the ratio between the conditioned and the unconditioned MEP is significantly lower than 1, this is referred to as 'inhibition', while a ratio significantly higher than 1 refers to 'facilitation'. Short-interval intracortical inhibition (SICI) is assessed by delivering a subthreshold (i.e. below MT) conditioning stimulus (CS) followed by a suprathreshold test stimulus (TS) delivered through the same TMS coil

(Kujirai et al., 1993). Depending on the ISI, two distinct phases of inhibition can be distinguished: SICI with an ISI of 1 ms, which is related to the membrane refractory period (Fisher et al., 2002) and is speculated to reflect extrasynaptic GABA tone (Stagg et al., 2011), and SICI with an ISI of 2–4 ms, reflecting short-lasting postsynaptic inhibition mediated through $GABA_A$ receptors (Ziemann et al., 2015), as identified by TMS-combined pharmacological studies (Di Lazzaro et al., 2000; Werhahn et al., 1999; Ziemann et al., 1996). Long-interval intracortical inhibition (LICI), combines two suprathreshold pulses (CS and TS), with an ISI ranging between 100 and 200 ms (Werhahn et al., 1999; McDonnell et al., 2006) and is suggested to be mediated by $GABA_B$ receptors (Werhahn et al., 1999; Roick et al., 1993; Siebner et al., 1998). The protocol for the identification of intracortical facilitation (ICF) is identical to SICI, with exception of the ISI, which ranges between 10 and 15 ms (Kujirai et al., 1993). Evidence from pharmacological studies has indicated that this protocol is mainly associated with glutamate receptor-mediated neurotransmission (Ziemann et al., 1996; Schwenkreis et al., 1999; Ziemann et al., 1998; Ziemann et al., 1995).

Whereas the TMS protocols described above advert to intracortical interactions, evoking inhibition or facilitation, mediated by respectively GABAergic and glutamatergic processes within M1, pharmacological studies have also revealed that interhemispheric interactions are associated with GABAergic inhibition (Irlbacher et al., 2007). Interhemispheric interactions between cortical brain regions and the contralateral M1 can be assessed by dual-site (ds)TMS (Ni et al., 2009). During dsTMS, a CS is applied over a region of one hemisphere, while a TS is applied over the M1 of the contralateral hemisphere. Although several dsTMS protocols are available, only the long-interval interhemispheric inhibition (LIHI) protocol is believed to contribute to the understanding of the underlying neurotransmitter systems. For example, LIHI with an ISI ranging between 40 and 60 ms is suggested to be mediated by $GABA_B$ receptors (Irlbacher et al., 2007).

Albeit the combination of TMS and EMG is primarily useful for understanding neurobiological processes at the level of M1, the combination of TMS and electroencephalography (EEG) is a technically challenging (Ilmoniemi and Kicic, 2010; Conde et al., 2019; Siebner et al., 2019; Belardinelli et al., 2019) and promising method for exploring the functionality of glutamatergic and GABAergic receptor-mediated neurotransmission within and beyond M1 (Amunts et al., 1996; X. Du et al., 2018; I. Premoli et al., 2014; I. Premoli et al., 2014; Rogasch et al., 2013; Opie et al. 2017). When combining TMS and EEG, TMS-evoked EEG potentials (TEPs) are measured. TEPs are generated by applying one or more TMS pulses to the cortex and measuring the TMS-induced changes in the scalp EEG signal. Again, pharmacological studies have been conducted to unravel the physiology underlying TEPs (for a review, see (Darmani and Ziemann, 2019)). Overall, it is suggested that earlier TEPs (<50 ms after TMS) resulting from spTMS such as the N45 (negative deflection at a latency of 45 ms) are linked to $GABA_A$, while later components (around 100 ms after TMS) such as the N100 seem to be associated to both $GABA_A$ or $GABA_B$-mediated inhibition, depending on the measurement site, respectively the non-stimulated or the stimulated hemisphere (Premoli et al., 2014). A recent study revealed that spTMS-evoked EEG potentials can be used to study the glutamatergic system as well (König et al., 2019). In addition to spTMS-evoked EEG potentials, the combination of ppTMS protocols such as SICI, LICI, and ICF with EEG, is suggested to yield surrogates of $GABA_A$, $GABA_B$ and glutamate receptor-mediated neurotransmission respectively (Premoli et al., 2014; Cash et al., 2017; Ferreri et al., 2011; Farzan et al., 2010; Daskalakis et al., 2008).

1.2. MRS

MRS provides a manner to non-invasively investigate molecular concentrations in tissues *in vivo* and identify metabolites involved in physiological and pathological processes. Magnetic resonance (MR) is based on the concept of nuclear spin, where nuclei with an odd number of protons or neutrons are studied. When placed in a strong magnetic field, i.e. an MR scanner, a radiofrequency (RF) pulse is applied to yield information about the biochemical structure surrounding the nucleus. The hydrogen (^{1}H) nucleus or proton is most commonly studied in MRS research on neurochemistry, as ^{1}H is the most abundant nucleus in the human body and therefore the hardware needed to acquire ^{1}H-MR spectra and software tools to process and quantify these data are widely available. For further in-depth reading on MRS principles and techniques and MRS detectable metabolites, we suggest e.g. (Buonocore and Maddock, 2015; De Graaf, 2019; Govind et al., 2000; Govindaraju et al., 2000; Maddock and Buonocore, 2012). In this review, we will focus on ^{1}H-MRS (Fig. 2).

^{1}H-MR spectra are usually acquired from a single cuboid volume (voxel) at a time, however, it is possible to acquire data from multiple voxels placed in parallel in one sequence in an simultaneous manner (Boer et al., 2015). MR spectroscopic imaging (MRSI) techniques are upcoming and can be used to acquire metabolic images to investigate larger brain areas or examine specific areas with a higher spatial resolution than is possible with single-voxel MRS (Ding and Lanfermann, 2015; Posse et al., 2013; Vidya Shankar et al., 2019). With ^{1}H-MRS the major spectral components *N*-acetyl aspartate (NAA), creatine, choline, and myo-inositol can be assessed in the brain *in vivo*, next to the combined signal of glutamate and glutamine, Glx. Assessment of e.g. glutamate and glutamine separately, gamma-aminobutyric acid (GABA), *N*-acetyl aspartyl glutamate (NAAG) and lactate is possible when requirements regarding magnetic field strength and/or RF pulse sequences are met.

1.2.1. NAA and NAAG

The NAA signal mostly represents the combined signals of NAA and NAAG and is therefore often referred to as total NAA (tNAA). NAA and NAAG are unevenly distributed across brain regions at concentrations of 8 to 16 millimolar (mM) and 0.6 to 3 mM respectively (Govindaraju et al., 2000; Pouwels and Frahm, 1998). Although there is no consensus about its exact function, changes in total NAA, particularly reductions, as observed with ^{1}H-MRS may reflect neuronal dysfunction that can be either permanent or reversible (Maddock and Buonocore, 2012; De Graaf, 2019; Moffett et al., 2007). NAA appears to decline with age and most consistently in gray matter (Cleeland et al., 2019). Reduced NAA levels have also been observed in several psychiatric disorders, however, psychopharmacological treatment seems to increase NAA levels (Paslakis et al., 2014). NAAG, the most abundant peptide neurotransmitter in the brain, is synthesized from NAA and glutamate (Arun et al., 2006; Cangro et al., 1987; Gehl et al., 2004; Neale et al., 2000). Similar to NAA, the exact role of NAAG remains unclear, although it has been suggested to be involved in excitatory neurotransmission and glutamate synthesis (Neale et al., 2000). The most prominent resonances of NAA and NAAG resonate closely to each other at 2.01 and 2.04 ppm respectively (Govindaraju et al., 2000). Consequently, high field strengths are typically required for detection of NAA and NAAG separately. Another way to separately detect NAA and NAAG is by spectral editing, where the 2.5 ppm resonance of NAA and the 2.6 ppm resonance of NAAG can be resolved, however, these resonance peaks are small and thus require relatively large MRS volumes and/or long scan times to achieve sufficient SNR (Edden et al., 2007).

1.2.2. Creatine and phosphocreatine

The creatine signals at 3.03 and 3.93 ppm represent the combined signals of creatine (Cr) and phosphocreatine (PCr) and are therefore usually referred to as total creatine (tCr). Creatine and phosphocreatine are present in all major cell types within the brain in concentrations of 4.5 to 6 mM and 4 to 5.5 mM respectively, with higher levels in grey matter (6.4 to 9.7 mM in total) compared to white matter (5.2 to 5.7 mM in total) (Maddock and Buonocore, 2012; Pouwels and Frahm, 1998; Erecinska and Silver, 1989; Wang and Li, 1998). Creatine and phosphocreatine are crucial in energy homeostasis and may serve as a buffer to

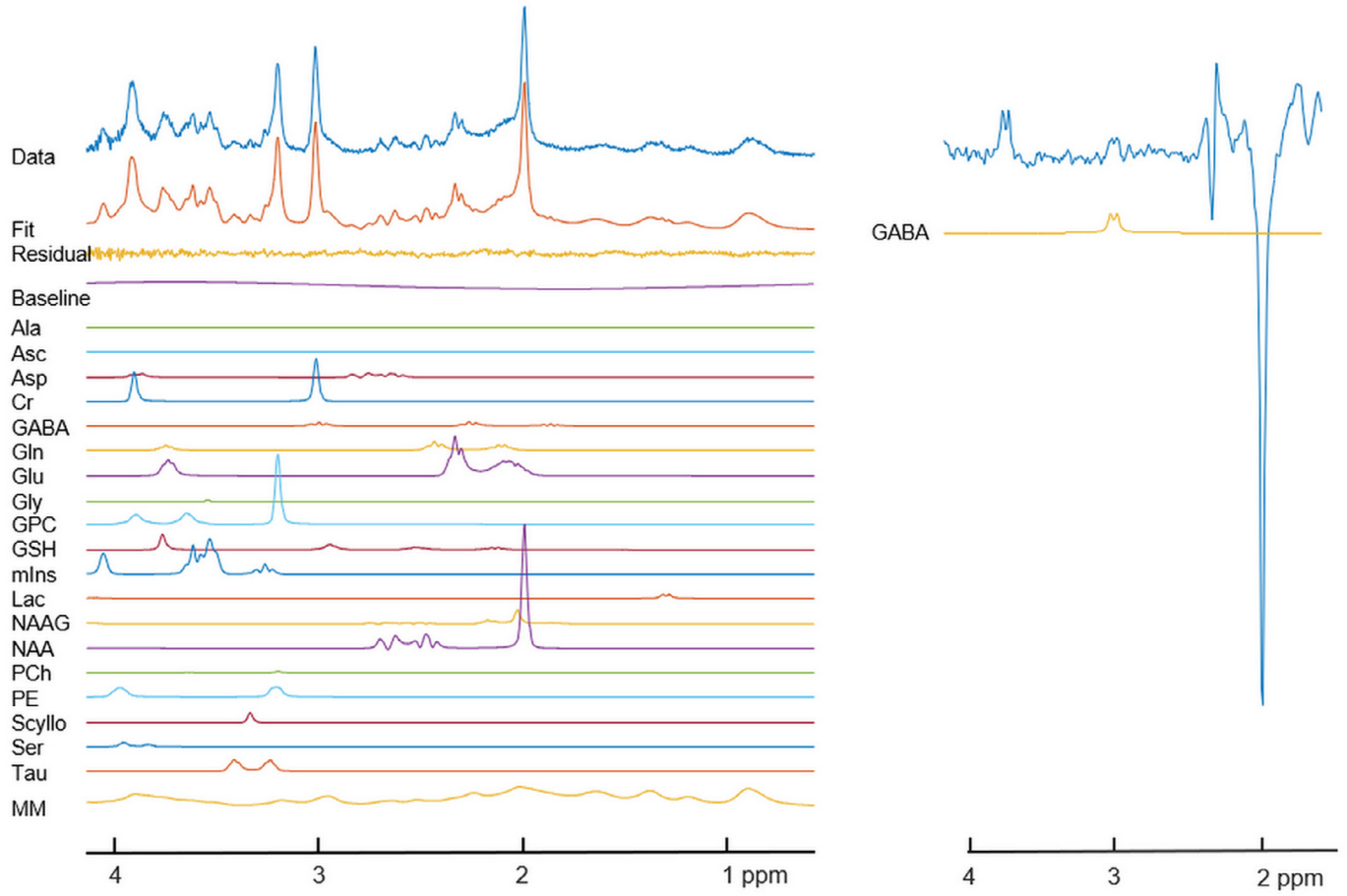

Fig. 2. Typical ^{1}H-MR spectra. Left: conventional ^{1}H-MR spectrum and fit. Right: MM-suppressed GABA-edited ^{1}H-MR spectrum and fit. Both spectra were acquired in the medial ACC using sLASER with a voxel size of 20 × 20 × 20 mm^3 at a magnetic field strength of 7T; for MM-suppressed GABA-editing, sLASER was combined with MEGA refocusing pulses at 1.5 and 1.9 ppm. Other sequence parameters include TR/TE=3700/30 ms and 16 averages for sLASER, and TR/TE=3700/74 ms and 32 averages for MEGA-sLASER. The sLASER spectrum was fitted with LCModel, the MEGA-sLASER spectrum was fitted with in-house developed software implemented in Matlab (Danish Research Centre for Magnetic Resonance). For clarity, the sLASER and MEGA-sLASER spectra are scaled differently. *Ala: alanine, Asc: ascorbate, Asp: aspartate, Cr: creatine, GABA: gamma-aminobutyric acid, Gln: glutamine, Glu: glutamate, Gly: glycine, GPC: glycerophosphorylcholine, GSH: glutathione, mIns: myo-inositol, Lac: lactate, NAAG: N-acetyl aspartyl glutamate, NAA: N-acetyl aspartate, PCh: phosphorylcholine, PE: phosphorylethanolamine, Scyllo: scyllo-inositol, Ser: serine, Tau: taurine, MM: macromolecules.*

maintain constant adenosine triphosphate (ATP) levels and as a shuttle diffusing energy from sites of net energy production to sites of net energy consumption (Maddock and Buonocore, 2012; De Graaf, 2019; Wallimann et al., 1992). The total creatine signal is often assumed to remain constant and thus used as an internal reference to normalize other metabolite signals. However, total creatine concentrations may change in disease (Gabbay et al., 2007; Mathews et al., 1995; Mirza et al., 2006; Tayoshi et al., 2009) and during the lifespan (see e.g. (Holmes et al., 2017; Levin et al., 2019; Marsman et al., 2013; Maudsley et al., 2012; Reyngoudt et al., 2012; Suri et al., 2017); see (Cichocka and Beres, 2018) for an overview of ^{1}H-MRS findings in brain development, maturation and aging).

1.2.3. Choline-containing compounds

The total choline (tCho) signal at 3.21 ppm arises from protons in free choline (Cho), glycerophosphorylcholine (GPC) and phosphorylcholine (PCh) with GPC and PCh being the main contributors, reflecting a total choline concentration of approximately 1 to 2 mM (Govindaraju et al., 2000; De Graaf, 2019). Choline-containing compounds are involved in phospholipid synthesis and degradation and the tCho signal is thus suggested to be associated with cell membrane turnover (Govindaraju et al., 2000; Maddock and Buonocore, 2012; De Graaf, 2019).

1.2.4. Myo-inositol

Myo-inositol (mIns) is a cyclic sugar alcohol and the most abundant isomer of inositol in mammalian tissues (Govindaraju et al., 2000; Maddock and Buonocore, 2012; De Graaf, 2019). Myo-inositol plays a role in the second messenger system, as an osmolyte and as an intermediate in phospholipid metabolism (Maddock and Buonocore, 2012). It is present in the brain in concentrations of 4 to 8 mM and gives rise to four resonance groups at 3.27, 3.52, 3.61 and 4.05 ppm (Govindaraju et al., 2000; R.A. De Graaf, 2019).

1.2.5. Glx, glutamate and glutamine

Glutamate (Glu) is the major excitatory neurotransmitter in the mammalian central nervous system and present in all cell types within the brain with concentrations typically ranging between 8 and 12 mM, although concentrations are different between grey and white matter (De Graaf, 2019). It is the precursor of GABA and a component in the synthesis of e.g. glutathione (GSH), a major antioxidant (De Graaf, 2019). Glutamate can be synthesized from its precursor glutamine, but also from α-ketoglutarate, a TCA-cycle intermediate. Glutamine (Gln) plays a role in the intermediary metabolism of amino acid neurotransmitters, most importantly glutamate and GABA, and is primarily located in astrocytes at concentrations of 2 to 4 mM (Maddock and Buonocore, 2012; De Graaf, 2019) (see (Bak et al., 2006;

Walls et al., 2015) for an overview of the glutamate/GABA-glutamine cycle). Because of their structural similarity, glutamate and glutamine have resonance peaks close to each other in the ^{1}H-MR spectrum at 3.75 and 3.77 ppm respectively and between 2.04 and 2.35 ppm and 2.12 and 2.46 ppm respectively (Govindaraju et al., 2000; De Graaf, 2019). Therefore, the combined glutamate and glutamine signal is often referred to as Glx. Separation of the glutamate and glutamine signals is unreliable at lower magnetic field strengths (De Graaf, 2019), but at field strengths of 7 tesla (T) or higher the glutamate and glutamine resonances at 2.35 and 2.46 ppm can be separated (Tkac et al., 2001). Short echo times (TE) improve the detection of glutamate and glutamine (Wilson et al., 2019). Mostly, MRS sequences already implemented on (clinical) scanners such as STEAM (Stimulated Echo Acquisition Mode) and PRESS (Point RESolved Spectroscopy) are applied, however, advanced MRS sequences such as sLASER (semi-Localized by Adiabatic SElective Refocusing) or SPECIAL (SPin-ECho full-Intensity Acquired Localized spectroscopy) may be beneficial for detection of glutamatergic compounds (Oz et al., 2020).

1.2.6. GABA

GABA is the major inhibitory neurotransmitter and present in the brain at a concentration of about 1 mM (De Graaf, 2019), although there are indications that concentrations differ between grey and white matter (see (Mikkelsen et al., 2016) for an overview). GABA has resonances at 1.89, 2.28 and 3.01 ppm which are all overlapped by more intense signals, hence spectral editing techniques are required for GABA detection (De Graaf, 2019).

Most commonly, Mescher-Garwood (MEGA) refocusing pulses (Mescher et al., 1998) are applied in ^{1}H-MRS sequences to resolve the GABA resonance at 3.01 ppm. In MEGA-editing of GABA, a refocusing pulse applied at 1.9 ppm is added to the MRS sequence. This pulse indirectly affects the 3.01 ppm GABA signal, since the 1.89 and 3.01 ppm GABA signals are coupled (see (Buonocore and Maddock, 2015) for a detailed explanation of J-coupling). When performing MRS experiments with (the ON experiment) and without (the OFF experiment) this pulse, the difference spectrum only contains signals affected by the pulse. Since there are no other molecules in the ^{1}H-MR spectrum with coupled signals at 1.9 and 3.0 ppm, the GABA signal will be the only signal that is refocused at 3.0 ppm.

Alternatively, double quantum filter (DQF) (Keltner et al., 1997) and two-dimensional (2D) ^{1}H-MRS (Ke et al., 2000) can be applied to measure GABA levels. The difference technique that is used in MEGA-editing is susceptible to instabilities due to e.g. motion in between ON and OFF experiments. DQF-MRS on the other hand, is a single-shot technique that filters out irrelevant uncoupled signals from the spectrum. However, it suffers from loss of at least half of the signal of interest (Bogner et al., 2017) which is a drawback when assessing weak signals such as GABA. 2D-MRS facilitates identification of signals by adding a spectral dimension, but suffers from lower SNR, increased acquisition times and susceptibility to instabilities (Bogner et al., 2017).

Ultra-high field strengths of 7T and up can be beneficial compared to lower clinical field strengths to measure GABA due to increased sensitivity and specificity. Where at lower field strengths the edited GABA signal is often contaminated by co-edited macromolecule (MM) signals, at higher field strengths it is easier to suppress these MM contributions. Both edited and non-edited sequences are used to measure GABA at 7T, however, while both methods show similar accuracy, editing shows higher precision (Hong et al., 2019).

1.2.7. Lactate

Lactate is the end product of anaerobic glycolysis and present in the brain at low concentrations of approximately 0.5 mM (Govindaraju et al., 2000; De Graaf, 2019). Increased lactate concentrations are typically observed in conditions of restricted blood flow (De Graaf, 2019); transient lactate increases have been observed following functional activation (Mangia et al., 2003; Prichard et al., 1991; Sappey-Marinier et al., 1992; Frahm et al., 1996) and hyperventilation (Posse et al., 1997; van Rijen et al., 1989). The lactate resonance at 1.31 ppm can be observed in short-TE ^{1}H-MR spectra, however, because of potential overlap with resonances from lipids, MM and threonine, it is best resolved using spectral editing techniques or long TE's (Govindaraju et al., 2000; De Graaf, 2019; De Graaf, 2019). In normal brain tissue, lipid contamination typically occurs with inadequate localization, otherwise the lactate signal at 1.31 ppm is only overlapped by threonine and MM resonances (De Graaf, 2019).

1.2.8. ^{1}H-MRS data handling

Several commercial and open-source software packages are available for quantification of metabolite levels from ^{1}H-MR spectra. Commonly used packages are e.g. LCModel (Provencher, 2001), jMRUI (Naressi et al., 2001), TARQUIN (Wilson et al., 2011) and Gannet (Edden et al., 2014). Regardless of the software however, several factors need to be considered when acquiring, processing and quantifying ^{1}H-MRS data (see (Oz et al., 2014) for in-depth reading). We describe the most common issues in short.

Technical limitations in ^{1}H-MRS data acquisition mainly concern RF transmit and receive performance which is related to the size and positioning of the head in the RF coil and the size, shape, positioning and anatomical location of the volume-of-interest (VOI) (Jansen et al., 2006). Next to that, local variations in susceptibility exist in the brain which can be counteracted by sufficient shimming, i.e. homogenization of magnetic field distribution across the region-of-interest (ROI) (Bhogal et al., 2017; Mandal, 2012). Motion may cause poor shimming and insufficient suppression of water and lipid signals and can thus affect ^{1}H-MRS signal quality (Jansen et al., 2006; Mandal, 2012). Considering the issues that can be encountered when acquiring ^{1}H-MRS data, continuous spectral quality assessment is needed to ensure sufficient data quality throughout a ^{1}H-MRS experiment or study. For an overview of spectral quality issues, see (Kreis, 2004). Before quantifying ^{1}H-MRS data, some processing is required to remove line-shape distortions, generally caused by magnetic field inhomogeneities or eddy currents induced by rapid switching of magnetic field gradients, and possible water and lipid signal residues, however, processing should be minimized to avoid adding bias (Oz et al., 2014; Jansen et al., 2006). Quantification of metabolite levels from ^{1}H-MR spectra requires a basis set of model spectra, acquired *in vitro* or simulated, that must be specifically generated for the used field strength, pulse sequence and acquisition parameters (Oz et al., 2014). Ideally, the basis set contains models of all ^{1}H-MRS detectable metabolites that are present in the tissue of interest as well as a macromolecular baseline to avoid overfitting of metabolite signals (Hofmann et al., 2002). The quality of the fit of the summed spectrum and individual metabolite spectra should be assessed by examining the residual signal and Cramèr-Rao lower bounds (CRLB) (Oz et al., 2014; Kreis, 2016). Lastly, sequence and vendor-specific issues need to be taken into account when acquiring, processing and quantifying ^{1}H-MRS data (Oz et al., 2014; Jansen et al., 2006).

2. Combining TMS and MRS

Over the last decade, there has been an increasing number of studies combining TMS and MRS. When applying TMS as a measurement tool, the combined TMS-MRS approach may reveal comprehensive and complementary information regarding metabolic processes at the level of the brain. Using a frameless stereotactic neuronavigation system to record the TMS coil position, MRS and TMS can be co-registered, assuring that approximately the same brain regions are studied (Hone-Blanchet et al., 2015), although there is no perfect convergence in terms of spatial resolution. Whereas TMS facilitates identification of functional aspects of the GABAergic and glutamatergic neurotransmitter system at the receptor level, MRS provides the possibility to detect a range of metabolites within a predefined volume of interest. A computer-based search of the PubMed database was carried out by both authors based

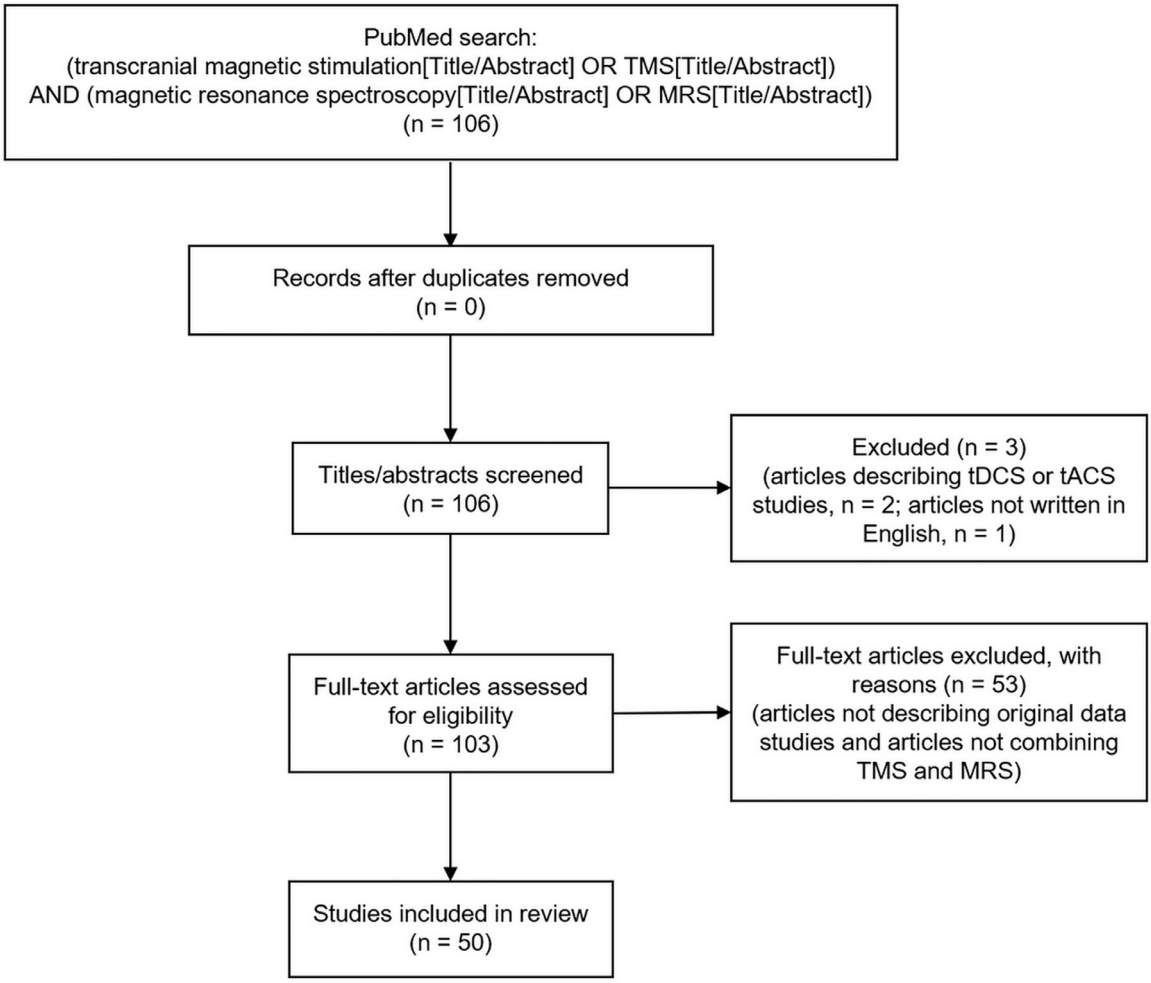

Fig. 3. Flow diagram of the literature search conducted on December 20, 2019, based on the PRISMA statement (Moher et al., 2009).

on the search term "(transcranial magnetic stimulation[Title/Abstract] OR TMS[Title/Abstract]) AND (magnetic resonance spectroscopy [Title/Abstract] OR MRS[Title/Abstract]). Studies not written in English and studies focusing on techniques that modify intrinsic activity without directly eliciting potentials in the targeted tissue (such as tDCS and tACS) were not included in this review. After screening a sample of 50 articles was included in this review. Here we review studies combining TMS and MRS, published up until December 20, 2019 (Fig. 3).

2.1. Healthy subjects

2.1.1. TMS as a measurement tool combined with MRS

See Table 1 for an overview of studies combining TMS as a measurement tool with MRS in healthy individuals.

2.1.1.1. GABA in M1. For $GABA_A$-mediated 'physiological' inhibition (Dyke et al., 2017) (i.e. SICI with ISI of 2.5 - 3 ms) several studies (Stagg et al., 2011; Dyke et al., 2017; Hermans et al., 2018; Mooney et al., 2017; Tremblay et al., 2013; Cuypers et al., 2020) indicate a lack of association between MRS and TMS measures, suggesting that both techniques probably measure complementary rather than similar features of the GABAergic neurotransmitter system. Interestingly, two studies (Stagg et al., 2011; Mooney et al., 2017) reported a relationship between GABA levels and SICI with an ISI of 1 ms, which was speculated to represent a GABAergic 'tone' generated by the activation of extrasynaptic $GABA_A$ receptors (Stagg et al., 2011). However, two other studies were not able to replicate this relationship between GABA levels and 1 ms SICI (Dyke et al., 2017; Hermans et al., 2018) and more research is desirable to clarify this finding. Although the exact mechanisms underlying 1 ms SICI remain to be identified, it can be assumed that MRS largely identifies pools of GABA which are linked to tonic instead of phasic inhibition and thus does not reflect specific activity at the level of the synapse.

In line with the absence of an association between $GABA_A$-mediated physiological inhibition and GABA levels, no relationship between measures of $GABA_B$-mediated inhibition and GABA levels has been observed so far (Stagg et al., 2011; Dyke et al., 2017; Hermans et al., 2018; Mooney et al., 2017; Tremblay et al., 2013).

Stagg and colleagues (2011) reported a positive correlation between GABA levels and the slope of the TMS input-output (IO) curve. Moreover, higher GABA levels were associated with a steeper slope. From a physiological point of view, this is a counterintuitive finding as the steepness of the slope reflects cortical excitability (Chen, 2000) and in particular the recruitment gain of α-motoneurons (Devanne et al., 1997). Therefore, a positive relationship between GABA levels (reflecting higher levels of inhibition) and the steepness of the slope seems to be unlikely. Nonetheless, this result was supported by findings from another study that revealed a positive correlation between MEP amplitude and GABA levels in M1 (Greenhouse et al., 2017). Currently, it is not clear how these results can be explained, but it is argued that glutamate likely plays a mediating role in this relationship (Stagg et al., 2011) and that higher GABA levels might compensate for a more excitable motor system (Greenhouse et al., 2017).

Table 1
Overview of studies combining MRS with TMS as a measurement tool in healthy individuals.

Study	Demographics		TMS		MRS						Significant findings TMS-MRS relation
	N	Age	Protocol	Region	FS	Sequence	Averages	TR/TE (ms)	Voxel size (mm^3)	Region	
Stagg et al. 2011	12	19–40	SICI LICI	l M1	3T	SPECIAL	128	2000/8.5	20 × 20 × 20	l M1	–
(Stagg et al., 2011)	12	19–46	SICI ICF LICI IO-curve	l M1	3T	SPECIAL	170	2000/8.5	20 × 20 × 20 20 × 20 × 20 20 × 30 × 20	l M1 r M1 OCC	Pos. correlation l M1 GABA/Cr - 1 ms SICI IO curve Pos. correlation l M1 Glu/Cr - MEP IO slope Pos. correlation l M1 GABA/Cr - MEP IO slope
Tremblay et al. 2013 (Tremblay et al., 2013)	24	20–38	SICI LICI CSP	l M1	3T	MEGA-PRESS	128	?	27 × 24 × 32	l M1	Pos. correlation Glx/Cr - CSP CSP predicts Glx/Cr
Dyke et al. 2017 (Dyke et al., 2017)	29	19–27	rMT Median MEP SI 1 mV IO-curve SICI LICI ICF	l M1	7T	STEAM	288	2000/17	20 × 20 × 20	l M1	Neg. correlation Glu/Cr - IO plateau Gln/Glu-and GABA/Glu-combined predict MEP at rMT Glu/Cr predicts ICF 10 ms Glu/Cr predicts IO plateau
Greenhouse et al. 2017 (Greenhouse et al., 2017)	24	21.9 ± 2.2	spTMS	r M1	3T	MEGA-PRESS	160	1500/68	30 × 30 × 30 25 × 40 × 25 25 × 40 × 25 30 × 30 × 30	r M1 r LPF r PM OCC	Pos. correlation l M1 GABA/Cr - MEP
Mooney et al. 2017 (Mooney et al., 2017)	15 16	20–31 62–83	CSP SICI LICI LCD	l M1	3T	MEGA-PRESS	96	1500–68	18 × 18 × 18	l M1	–
Du et al. 2018 (X. Du et al., 2018)	21	21–61	TEP-N100	l PFC l M1 vertex	3T	STEAM MEGA-PRESS	256 256	2000/6.5 2000/68	40 × 30 × 20	m PFC	Neg. correlation Glu/GABA - supra-threshold l PFC evoked N100 at FZ Neg. correlation [Glu] - supra-threshold l PFC evoked N100 at FZ Pos. correlation [GABA] - supra-threshold l PFC evoked N100 at FZ
Du et al. 2018 (X. Du et al., 2018)	20	20–62	TEP	post. cerebellum l PFC	3T	STEAM MEGA-PRESS	256 256	2000/6.5 2000/68	40 × 30 × 20	m PFC	Pos. correlation Glu/GABA - supra-threshold cerebellar evoked PFC synchrony Neg. correlation [GABA] - supra-threshold cerebellar evoked PFC synchrony Pos. correlation Glu/GABA - sub-threshold cerebellar evoked PFC synchrony Neg. correlation [GABA] - sub-threshold cerebellar evoked PFC synchrony Pos. correlation Glu/GABA - supra-threshold L PFC evoked PFC synchrony Neg. correlation [GABA] - supra-threshold L PFC evoked PFC synchrony Pos. correlation [Glu] - supra-threshold L PFC evoked PFC synchrony Pos. correlation Glu/GABA - sub-threshold L PFC evoked PFC synchrony Neg. correlation [GABA] - sub-threshold L PFC evoked PFC synchrony
Hermans et al. 2018 (Hermans et al., 2018)	28 28	19–34 63–74	IO-curve IO-curve SICI ICF LICI SIHI LIHI	l M1 r M1 l M1 l M1 l M1 l M1 -> *r* M1 l M1 -> *r* M1	3T	MEGA-PRESS	40	2000/68	30 × 30 × 30	l SM1 OCC	–

FS: field strength, l: left, LCD: late cortical disinhibition, LPF: lateral prefrontal, m: medial, OCC: occipital, PM: premotor, post.: posterior, PRESS: point resolved spectroscopy, r: right, SM1: sensorimotor cortex, SIHI: short-latency interhemispheric inhibition, SPECIAL: spin-echo full-intensity acquired localized spectroscopy, STEAM: stimulated echo acquisition mode, TR: repetition time.

2.1.1.2. Glx, glutamate and glutamine in M1. Whereas in M1 hardly any association between GABA levels and TMS measures (except for SICI 1 ms and IO curve) are reported, several studies identified a link between Glx or glutamate with TMS (Stagg et al., 2011; Dyke et al., 2017; Tremblay et al., 2013). In one study glutamate levels were positively associated with the steepness (Stagg et al., 2011) of the IO curve. The authors speculated that a higher glutamate level reflects increased presynaptic glutamate storage and thus more glutamate release with increasing TMS intensity. Another study found a negative correlation between glutamate levels and the plateau of the TMS IO curve (Dyke et al., 2017). Although one would expect that a higher glutamate level would be associated with a higher plateau, reflecting higher excitability, this relationship might be more complex. Indeed, Devanne et al., (1997) argued that the plateau is not reflected by purely excitatory components, but more likely by the balance between excitatory and inhibitory components of the corticospinal volley (Devanne et al., 1997). Furthermore, there is evidence that the slope and the plateau of the TMS IO curve are distinct measures, relating to different mechanisms (Kouchtir-Devanne et al., 2012).

One study showed that Glx was positively related to CSP (Tremblay et al., 2013). As CSP is thought to reflect GABA receptor-mediated inhibition (Ziemann et al., 2015), a relationship between Glx and CSP is rather unexpected. Nonetheless, there is supporting evidence showing that glutamate and $GABA_B$-receptors closely interact in regulating the excitability balance in the brain (see, (Kantamneni, 2015) for a review). More specific, $GABA_B$-receptors seem to affect the expression, activity and signaling of glutamate receptors, while NMDA receptors are capable to regulate $GABA_B$ receptor expression, signaling and function (Kantamneni, 2015).

Another study revealed a positive relationship between glutamate and ICF, a measure that is associated with excitability and in particular mainly with glutamate receptor-mediated neurotransmission (Ziemann et al., 1996; Schwenkreis et al., 1999; Ziemann et al., 1998; Ziemann et al., 1995). It should be noted that this relationship was only significant for ICF with an ISI of 10 ms. There was no relationship between glutamate and ICF with an ISI of 12 ms, a result consistent with previous work (Stagg et al., 2011). Unlike for SICI, there is currently no evidence for a distinction based on different ISI's and it remains unclear why differences were found between both TMS paradigms.

2.1.1.3. Metabolites in regions beyond M1. Du et al. (2018) suggested that the N100 peak, as determined by EEG, represents the balance between local levels of GABA and glutamate (Du et al., 2018). They recorded TEPs at the FZ electrode resulting from supra-threshold spTMS over the left prefrontal cortex (PFC) and found that 46% of the individual variance in the N100 was significantly predicted by the ratio between glutamate and GABA in the medial PFC. Moreover, high glutamate and low GABA levels predicted a higher N100 amplitude, while low glutamate and high GABA levels predicted a lower N100 amplitude. The authors indicated that electrical transmissions evoked by TMS at left PFC are influenced by local glutamate and GABA levels. In another TEP study of the same group, TMS was applied over the cerebellar cortex or left PFC with the aim to modulate cerebellar-prefrontal connectivity (Du et al. 2018). The results indicated that GABA levels in the medial PFC were negatively correlated to bilateral prefrontal synchrony in the theta to gamma frequency range after cerebellar TMS, and in the theta to low beta frequency range after stimulation of the left prefrontal cortex. Furthermore, there was a positive correlation between glutamate levels in medial PFC and bilateral prefrontal synchrony in theta to low beta frequency range after TMS over the left prefrontal cortex. These results indicate that regional metabolite levels are likely to mediate interregional network interactions.

2.1.2. TMS as an interventional approach combined with MRS

See Table 2 for an overview of studies combining interventional TMS with MRS in healthy individuals.

2.1.2.1. rTMS. In healthy volunteers, a single session of cTBS was sufficient to modulate GABA levels in the targeted region. Specifically, GABA levels in primary visual cortex (V1) (Allen et al., 2014) and M1 (Stagg et al., 2009) were increased after cTBS over these regions. In contrast, Glx levels were not modulated after cTBS over M1 (Stagg et al., 2009). Interestingly, two studies reported that modulation of metabolites after a single iTBS session was associated with functional connectivity strength changes, assessed with resting-state functional magnetic resonance imaging (fMRI) (Iwabuchi et al., 2017; Vidal-Pineiro et al., 2015). One study reported an increase in the GABA/Glx ratios in anterior cingulate cortex (ACC) and both dorsolateral prefrontal cortices (DLPFC's) after iTBS over left DLPFC (Iwabuchi et al., 2017). Moreover, changes in GABA/Glx ratios in DLPFC were associated with a decreased connectivity between DLPFC and right anterior insula. Another study showed an increase in GABA levels in the posteromedial default mode network (DMN) regions after iTBS administered to the left inferior parietal lobe (IPL) (Vidal-Pineiro et al., 2015). Additionally, iTBS-induced GABA level changes were associated with baseline functional connectivity strength between the left IPL and posteromedial DMN regions. In a study conducted in a population of active duty military members, low-frequency rTMS over left DLPFC altered the relationship between metabolites (tNAA, Glx and Cho) and pre to post metabolite ratios were negatively associated with baseline metabolite ratio levels (Bridges et al., 2018). However, rTMS did not change absolute metabolite levels. This result was partly supported by another study that reported no changes in tNAA, Cho and Cr, but identified changes in Glx levels in left DLPFC (reduction after one session, but return to baseline after five sessions) and more remote brain regions (right DLPFC and left cingulate cortex; increase after five sessions) after high-frequency rTMS over left DLPFC (Michael et al., 2003). A recent pilot study performed with a 7T scanner, evaluated the effect of low-frequency (1 Hz) rTMS over the left M1 on levels of several metabolites and functional connectivity in young healthy males (Grohn et al., 2019). The results revealed a decrease of GABA levels in both the stimulated and the non-stimulated M1, and an increase in tCr and a decrease in aspartate (Asp) in the stimulated M1. No rTMS-induced changes were reported for other metabolites nor for connectivity metrics.

2.1.2.2. PAS. Coordinated pharyngeal peripheral and cortical stimulation successfully increased pharyngeal excitability assessed by spTMS (Singh et al., 2009). Additionally, glutamate levels decreased in the stimulated M1. Another study of the same group revealed an increased blood-oxygen-level-dependent (BOLD) response at the site of stimulation and at contralateral regions, using a shorter but comparable PAS protocol (Michou et al., 2015). Although there was a trend towards an increase, contralateral GABA levels did not change significantly after PAS.

2.2. Patient populations

2.2.1. TMS as a measurement tool combined with MRS

TMS and MRS have been combined to study a variety of pathological conditions, such as sports-related concussion (Tremblay et al., 2014), depression (Lewis et al., 2016), amyotrophic lateral sclerosis (ALS) (Kaufmann et al., 2004; Pohl et al., 2001), primary lateral sclerosis (PLS) (Zhai et al., 2003), spinal cord injury (SCI) (Puri et al., 1998) and in patients with multiple sclerosis (MS) (see Table 3A) (Zeller et al., 2011). In the majority of the studies, spTMS was applied over M1 or the vertex as a control with respectively a figure-of-eight or a round coil.

In a sample of football players who had experienced one or more sports-related concussions, the effect of concussion on multiple neuroimaging and TMS metrics was investigated (Tremblay et al., 2014). The results of this work showed that football players who experienced one or more concussions did not differ from football players who never experienced a concussion in any of the collected metrics. More

Table 2
Overview of studies combining MRS with interventional TMS in healthy individuals.

Study	Demographics		TMS			MRS						Significant findings TMS-MRS relation
	N	Age	Protocol	Intensity	Region	FS	Sequence	Averages	TR/TE (ms)	Voxel size (mm^3)	Region	
Michael et al. 2003 (Michael et al., 2003)	7 (real) 5 (sham)	47±14 45.2 ± 12	rTMS (20 Hz) 800 pulses 1/5 sessions	80% rMT	l DLPFC	1.5T	STEAM	128	2500/20	3375	l DLPFC r DLPFC l ACC	Lower l DLPFC [Glx] after 1 real rTMS compared to preTMS Neg. correlation l DLPFC [Glx] preTMS - 24 h after 5 real rTMSHigher r DLPFC [Glx] after 5 real rTMS compared to after 1 real rTMS Neg. correlation r DLPFC [Glx] preTMS - after 1 real rTMS Higher l ACC [Glx] after 5 real rTMS compared to 24 h after 5 sham rTMS Neg. correlation l ACC [Glx] preTMS - after 1/5 real rTMS
Singh et al. 2009 (Singh et al., 2009)	15	21–56	PAS 90 pulses 1 session	120% rMT	pharyngeal MC	3T	PRESS	128	2000/32	20 × 20 × 20	M1 contral. OCC	Lower M1 Glu/NAA after PAS
Stagg et al. 2009 (Stagg et al., 2009)	16	21–44	cTBS 600 pulses 1 session	80% AMT	l M1	3T	MEGA-PRESS	192?	?/68	20 × 20 × 20	l M1	Higher GABA/NAA after cTBS
Allen et al. 2014 (Allen et al., 2014)	18	21–35	cTBS 600 pulses 2 sessions	80% rMT	V1	3T	MEGA-PRESS	512	1800/68	30 × 30 × 30	V1	Higher [GABA] after real cTBS compared to sham cTBS
Michou et al. 2015 (Michou et al., 2015)	11	35 ± 9	PAS ISI=100 ms 2 sessions	120% rMT	l pharyngeal MC r pharyngeal MC	3T	MEGA-PRESS	192	2000/68	32 × 32 × 32	l M1 r M1 contral. OCC	–
Vidal-Piñeiro et al. 2015 (Vidal-Pineiro et al., 2015)	36	23.5 ± 2.0	iTBS cTBS 600 pulses 1 session	80% aMT 80% aMT	l IPL	3T	MEGA-PRESS	256	1500/68	30 × 20 × 15	l IPL PCC	Higher PCC GABA/Cr after real iTBS compared to sham iTBS and cTBS Pos. correlation PCC GABA/Cr after iTBS - pre-TBS funcitonal connectivity between stimulated area and posteromedial cortex Neg. correlation PCC Glx/Cr after iTBS - rs-fMRI connectivity
Iwabuchi et al. 2017 (Iwabuchi et al., 2017)	28	19–50	iTBS 600 pulses 1 real 1 sham	80% rMT	l DLPFC	3T	PRESS	128	2500/105 (TE_1=15 ms)	32 × 16 × 16 30 × 30 × 15	l DLPFC ACC	Lower DLPFC and ACC GABA/Glx after real iTBS compared to sham Neg. correlation DLPFC GABA/Glx - DLPFC-rAI effective connectivity for real iTBS
Bridges et al. 2018 (Bridges et al., 2018)	11	18–42	rTMS (1 Hz) 1200 pulses 1 session	100% rMT	l DLPFC	1.5T	PRESS	4	1500/135	20 × 20 × 20	l DLPFC	Interaction Cho/Cr and condition with no main effects Pos. correlation Cho/Cr - tNAA/Cr (real + sham) Pos. correlation tNAA/Cr - Glx/Cr (sham) Pos. correlation Glx/Cr - Cho/Cr (real) Neg. correlation post-pre stimulation Glx/Cr difference - baseline Glx/Cr (real + sham) Neg. correlation post-pre stimulation tNAA/Cr difference - baseline tNAA/Cr (real) Neg. correlation between post-pre stimulation Cho/Cr differences and baseline Cho/Cr for sham condition only
Grohn et al. 2019 (Grohn et al., 2019)	7	21–40	rTMS (1 Hz) 1200 pulses 1 session	90% rMT	l M1	7T	sLASER	64	9000/28	24 × 22 × 17	l M1 r M1	Higher [GABA], [Glu], [Gln], [tCho], [mIns], [GSH], [NAA] in R M1 compared to L M1 at baseline Higher L M1 [GABA] and [tCr] after rTMS Lower R M1 [GABA] after rTMS Lower L M1 [Asp] after rTMS

Contral.: contralateral, ISI: interstimulus interval, PCC: posterior cingulate cortex.

Table 3A
Overview of studies combining MRS with TMS as a measurement tool in patient populations.

Study	Demographics			TMS		MRS						Significant findings TMS-MRS relation
	Population	N	Age	Protocol	Region	FS	Sequence	Averages	TR/TE (ms)	Voxel size (mm^3)	Region	
Puri et al. 1998 (Puri et al., 1998)	SCI ctrl	6 5	30–66	spTMS	l M1 r M1	1.5T	CSI	512	1500/?	20 × 15 × 15	M1 OCC	–
Pohl et al. 2001 (Pohl et al., 2001)	ALS	49	56.3 ± 14.1	CMCT	Cz	1.5T	PRESS	128	2000/272	40 × 30 × 25	M1	Lower NAA/Cho in hemispheres with cortical inexitability
Zhai et al. 2003 (Zhai et al., 2003)	PLS ctrl	25 22	45.72±7.89 53.5 ± 12.0	CMCT spTMS	M1	1.5T	MRSI	?	?/280	7.5 × 7.5 × 15	l M1 hand r M1 hand l M1 leg r M1 leg l int. capsule r int. capsule l pons r pons	Neg. correlation finger tapping speed - TMS threshold (pt + ctrl combined) Pos. correlation finger tapping speed - NAA/Cr (pt + ctrl combined)
Kaufmann et al. 2004 (Kaufmann et al., 2004)	ALS	164	?	CMCT	Cz	1.5T	PRESS	96	2000/272	20 × 20 × 20	l prec. gyrus r prec. gyrus	Lower NAA/Cr in pt with UMN signs compared to pt without UMN signs Association presence of UMN signs - abnormal NAA/Cr
Tremblay et al. 2014 (Tremblay et al., 2014)	Concussion ctrl	16 14	22.00±1.09 22.03±1.08	CSP LICI	l M1	3T	MEGA-PRESS	?	?	27 × 24 × 32	l M1	–
Lewis et al. 2016 (Lewis et al., 2016)	MDD	24	11–18	rMT CSP SICI ICF	l M1	3T	PRESS	128	2000/80	20 × 20 × 20	m ACC l M1	Pos. correlation rMT - L M1 [Glx] Pos. correlation ICF-10 - ACC [Glx] Pos. correlation ICF-20 MEP - ACC [Glx]

ALS: amyotrophic lateral sclerosis, CSI: chemical shift imaging, ctrl: control, int.: internal, MDD: major depressive disorder, mTBI: mild traumatic brain injury, PLS: primary lateral sclerosis, prec.: precentral, SCI: spinal cord injury.

specifically, there were no differences in GABA levels, glutamate levels, CSP, LICI or measures of cortical thickness assessed in the left M1 (Tremblay et al., 2014).

A study by Lewis et al. (2016) showed a positive correlation between Glx levels in the left M1 and the resting motor threshold, a TMS measure of cortical excitability, in adolescents with depressive symptoms (Lewis et al., 2016). Additionally, a positive relationship between Glx levels in the medial ACC and ICF measures at left M1 was found. These results indicate a link between Glx levels and TMS-derived excitability metrics in adolescents with depression.

Two studies conducted in ALS patients showed that MRS measures of NAA in M1, TMS-derived CMCT and their combination have potential for early diagnosis of ALS. Measures obtained from both MRS and TMS showed to be sensitive markers in the detection of upper motor neuron (UMN) involvement in ALS (Kaufmann et al., 2004; Pohl et al., 2001).

In patients with PLS, corticospinal excitability, CMCT and metabolite levels in the motor cortex were investigated (Zhai et al., 2003). PLS patients with ascending symptom progression showed absence of MEPs and a reduced NAA/Cr ratio (an indicator of neuronal atrophy) in the motor cortex as compared to healthy controls.

Finally, the MRS-derived NAA/Cr ratio was shown to be a prognostic marker of recovery in patients with SCI (Puri et al., 1998).

2.2.2. spTMS as a tool to interfere with neural processing combined with MRS

In patients with MS and healthy controls, spTMS was used as a tool to interfere with neural processing of brain regions (including contra- and ipsilateral M1, ipsilateral dorsal premotor cortex (PMd) and a mid-occipital region) during the performance of a simple reaction time task (see Table 3B) (Zeller et al., 2011). Whereas spTMS over M1 to the performing hand increased reaction time in both patients with MS and healthy controls, administration of spTMS to the ipsilateral M1 and PMd increased reaction time only in patients with MS, but not in healthy controls. This finding can be explained in terms of a compensatory role for ipsilateral motor-related regions to compensate for dysfunction and as an adaptive response to chronic brain injury in patients with MS (Zeller et al., 2011). In addition, patients with MS had a lower NAA/Cr ratio in the corpus callosum as compared to healthy controls.

2.2.3. TMS as an interventional approach combined with MRS

2.2.3.1. Depression. Several studies identified the effects of multiple high-frequency rTMS sessions (Baeken et al., 2017; Croarkin et al., 2016; Dubin et al., 2016; Erbay et al., 2019; Levitt et al., 2019; Luborzewski et al., 2007; Zheng et al., 2015; Zheng et al., 2010) on symptom severity and metabolites in patients with depression (see Table 4A). In all studies, the left DLPFC was targeted. VOIs for measuring metabolic changes were located in the prefrontal cortex. Two studies identified an increase in GABA levels in the mPFC (Dubin et al., 2016) and left DLPFC (Levitt et al., 2019) after rTMS, while a third study showed a positive relationship between rTMS-induced GABA levels and clinical improvement (Baeken et al., 2017). GABA increase was more evident in responders to rTMS (defined by a reduction on the Hamilton Depression Rating Scale (HAMD) score) as compared to non-responders (Levitt et al., 2019). One study reported an increase in the glutamine/glutamate ratio in ACC and left DLPFC (Croarkin et al., 2016) and found that these changes were associated with decreased symptom severity. Along the same lines, another study found that rTMS increased the glutamine/creatine ratio in the left DLPFC (Erbay et al., 2019), however, these changes were not related to changes in the HAMD score. It has to be noted that in patients with depression, baseline glutamatergic levels in the left DLPFC are lower as compared to healthy controls (Baeken et al., 2017) and that responders to rTMS have mainly lower baseline levels (Luborzewski et al., 2007). Similar to glutamatergic levels, baseline NAA, choline and myo-inositol (MI) levels were lower in patients with depression as compared to healthy controls (Zheng et al., 2015; Zheng et al., 2010). However, NAA in the left ACC (Zheng et al.,

Table 3B
Overview of studies combining MRS with TMS as a tool to interfere with neural processing in patient populations.

Study	Demographics			TMS		MRS					Significant findings TMS-MRS relation	
	Population	N	Age	Protocol	Region	FS	Sequence	Averages	TR/TE (ms)	Voxel size (mm^3)	Region	
Zeller et al. 2011 (Zeller et al., 2011)	MS ctrl	26 26	23–60	spTMS	l M1 r M1 r PMd MO	1.5T	PRESS	96	3000/30	80,000	corpus callosum	–

MS: multiple sclerosis.

Table 4A
Overview of studies combining MRS with interventional TMS in patient populations.

Study	Demographics			TMS			MRS						Significant findings TMS-MRS relation
	Population	N	Age	Protocol	Intensity	Region	FS	Sequence	Averages	TR/TE (ms)	Voxel size (mm^3)	Region	
Luborzewski et al. 2007 (Luborzewski et al., 2007)	MDD	17	28–61	rTMS (20 Hz) 2000 pulses 10 sessions	100% rMT	l DLPFC	3T	PRESS	256 128	3000/80	20 × 20 × 20 25 × 40 × 20	l DLPFC ACC	Lower DLPFC [Glu] and [tCho] in responders as compared to non-responders Higher DLPFC [Glu] after rTMS in responders Lower DLPFC [Glu] after rTMS in non-responders Higher DLPFC [tCho] after rTMS in responders
Zeller et al. 2010 (Zeller et al., 2010)	MS ctrl	22 22	21–59	PAS ISI=25 ms	130% rMT	dom. M1	?	?	?	?	?	?	
Zheng et al. 2010 (Zheng et al., 2010)	MDD ctrl	19 (real) 15 (sham) 28	18–37	rTMS (15 Hz) 3000 pulses 20 sessions	110% rMT	l DLPFC	3T	CSI	3	1700/30	10 × 10 × 15 (VOI) 80 × 80 × 15 (ROI)	l PFC r PFC	Higher l PFC mIns/Cr in responders after rTMS as compared to baseline
Fregni et al. 2011 (Fregni et al., 2011)	Visceral pain	8 (real) 9 (sham)	18–65	rTMS (1 Hz) 1600 pulses 10 sessions	70% MSO	r S2	3T	PRESS	128	3000/35	20 × 20 × 20	l S2 r S2	Neg. correlation between pain intensity change and baseline [Glu] in l and r S2 regardless of treatment group Higher [Glu] in l and r S2 after real rTMS Pos. corelation between pain intensity change and [Glu} change in l and r S2 after real rTMS
Marjanska et al. 2013 (Marjanska et al., 2013)	Upper limb dystonia ctrl	15 14	22–63 23–68	rTMS (5 Hz) 1800 pulses	90% rMT	dom. M1	3T	MEGA-PRESS	256	3000/68	28.8 ml 20.8 ml 27.6 ml	bil. MC bil. nc. lentiformis OCC	Lower dominant MC [NAA] after rTMS in both groups Lower dominant MC [Glx] after rTMS in both groups Higher dominant MC [GABA] after rTMS in controls Lower dominant MC [GABA] after rTMS in patients
Zheng et al. 2015 (Zheng et al., 2015)	TRD ctrl	18 (real) 14 (sham) 28	26.9 ± 6.4 26.9 ± 4.3 27.6 ± 5.1	rTMS (15 Hz) 3000 pulses 20 sessions	110% rMT	l DLPFC	3T	CSI	3	1700/30	10 × 10 × 15 (VOI) 80 × 80 × 15 (ROI)	l ACC r ACC	Higher L ACC NAA/Cr after real rTMS as compared to baseline in responders Pos. correlation between relative WCST improvement of perseverative errors and relative l ACC NAA/Cr change after real rTMS
Croarkin et al. 2016 (Croarkin et al., 2016)	MDD	10	13–17	rTMS (10 Hz) 3000 pulses 30 sessions	120% rMT	l DLPFC	3T	PRESS 2DJ-PRESS	128 16 steps	2000/80 2000/35–195	20 × 20 × 20	l DLPFC ACC	Higher ACC Gln/Glu (PRESS) and DLPFC Gln/Glu (2DJ) after rTMS and after 6-month follow-up as compared to baseline Higher ACC Gln/Glu (PRESS) and DLPFC Gln/Glu (PRESS and 2DJ) after 6-month follow-up as compared to after rTMS
Dlabac-de Lange et al. 2016 (Dlabac-de Lange et al., 2017)	SZ	11 (real) 13 (sham)	39.4 ± 11.6 32.6 ± 9.9	rTMS (10 Hz) 2000 pulses 30 sessions	90% rMT	l DLPFC r DLPFC	3T	PRESS	128	2000/144	20 × 20 × 20	l DLPFC	Neg. association between [Glx] change after rTMS and treatment condition Pos. association between [Glx] change after rTMS and treatment condition x baseline [Glx] interaction
Dubin et al. 2016 (Dubin et al., 2016)	MDD	23	21–68	rTMS (10 Hz) 3000 pulses 25 sessions	80 - 120% rMT	l DLPFC	3T	MEGA-PRESS	?	?/68	25 × 25 × 30	m PFC	Higher GABA/H2O after rTMS as compared to baseline in all subjects Higher GABA/H2O after rTMS as compared to baseline in responders Higher GABA/H2O after rTMS as compared to baseline in responders without comorbidities Pos. association between relative GABA/H2O change after rTMS and age Pos. association between relative GABA/H2O change after rTMS and male sex

(*continued on next page*)

Table 4A (*continued*)

Study	Demographics Population	N	Age	TMS Protocol	Intensity	Region	MRS FS	Sequence	Averages	TR/TE (ms)	Voxel size (mm^3)	Region	Significant findings TMS-MRS relation
Qiao et al. 2016 (Qiao et al., 2016)	Alcohol-dependency	18 (real) 20 (sham)	49 (median) 48 (median)	rTMS (10 Hz) 800 pulses 20 sessions	80% rMT	r DLPFC	1.5T	PRESS	128	1500/35	20 × 20 × 20	l hipp. r hipp.	Higher l and r hipp. NAA/Cr and Cho/Cr after rTMS as compared to baseline in real and sham group Greater increase in l and r hipp. NAA/Cr after real rTMS as compared to sham rTMS
Baeken et al. 2017 (Baeken et al., 2017)	TRD ctrl	18 18	47.17±12.54 45.17±12.34	rTMS (20 Hz) 1560 pulses 20 sessions	110% rMT	l DLPFC	3T	PRESS	128	2000/40	15 × 15 × 15 30 × 30 × 15	l DLPFC r DLPFC l ACC	Neg. correlation between pre-post rTMS Beck Depression Inventory (BDI-II) change and pre-post rTMS L DLPFC [GABA] change
Cacace et al. 2017 (Cacace et al., 2017)	Tinnitus	30	24–80	rTMS (1 Hz) 1200 pulses 5 sessions	110% rMT	aud. cortex l temp. lobe	3T	STEAM	256	1500/72	15 × 20 × 15	l aud. cortex r aud. cortex	Greater l aud. cortex [Glu] change after real rTMS as compared to sham rTMS Greater l aud. cortex [Glu] change after real rTMS as compared to R auditory cortex [Glu] change after sham rTMS Greater l aud. cortex [Glu] change after real rTMS as compared to r auditory cortex [Glu] change after real rTMS Pos. correlation between r aud. cortex [Glu] and T&H after real rTMS Neg. correlation between r aud. cortex [Cho] and SEB after sham rTMS Pos. correlation between l aud. cortex [NAA} after real rTMS and r aud. cortex [Cho] after sham rTMS Pos. correlation between reduction of tinnitus loudness and [Glu] decrease in stimulated hemisphere after real rTMS
Di Lazzaro et al. 2017 (Di Lazzaro et al., 2017)	ALS	3	43–78	cTBS 600 pulses 120 sessions	80% aMT	bil. M1	3T	PRESS MEGA-PRESS	? 320	? 2000/68	30 × 30 × 20	l M1 l WM (caudal to M1) pons tegmen l M1	–
Hone-Blanchet et al. 2017 (Hone-Blanchet et al., 2017)	Substance use disor-der(case study)	1	19	rTMS (1 Hz) 600 pulses 5 sessions	120% rMT	r DLPFC	3T	MEGA-PRESS	?	?	30 × 30 × 30	r DLPFC r striatum r ACC	Higher [Glx] in all regions after rTMS Higher [NAA] in DLPFC and striatum after rTMS
Erbay et al. 2019 (Erbay et al., 2019)	MDD	18	43.38±11.14	rTMS (10 Hz) 3000 pulses 20 sessions	?	l DLPFC	3T	PRESS	?	2000/30	15 × 20 × 15	l DLPFC	Higher NAA/Cr, GSH/Cr and Glc/Cr after rTMS as compared to baseline
Flamez et al. 2019 (Flamez et al., 2019)	PD	17	70.94±10.17	rTMS (1 Hz) 1000 pulses 1 real 1 sham	90% rMT	r preSMA	3T	PRESS	128	2000/38	20 × 20 × 20	r preSMA	Neg. correlation between disease duration and tCho/tCr change after one real rTMS session Neg. correlation between disease duration and tCho/tCr real vs.sham difference
Fried et al. 2019 (Fried et al., 2019)	Diabetes 2 Pre-diabetes Non-diabetic	17 14 9	50–87	spTMS iTBS 600 pulses 1 session	120% rMT 80% aMT	l M1	3T	PRESS	128	2000/35	20 × 20 × 20	l M1	Pos. correlation between MEP and Glu/tCr in type 2 diabetes patients

(*continued on next page*)

Table 4A (*continued*)

Study	Demographics Population	N	Age	TMS Protocol	Intensity	Region	MRS FS	Sequence	Averages	TR/TE (ms)	Voxel size (mm^3)	Region	Significant findings TMS-MRS relation
Levitt et al. 2019 (Levitt et al., 2019)	MDD	26	38.40±13.8	rTMS (10 Hz) 3000 pulses 30 sessions	80 - 120% rMT	l DLPFC r DLPFC	3T	MEGA-PRESS	192	2000/68	30 × 20 × 10 (size adjusted to maximize GM content)	l DLPFC	Higher [GABA] after rTMS compared to baseline in total sample Higher [GABA] after rTMS compared to baseline in responders Pos. correlation between [Glx] and [GABA] at baseline and after rTMS in total sample More rTMS responders among patients not taking GABA agonists (N = 14) as compared to patients taking GABA agonists (N = 12) Greater decrease in depressive symptoms after rTMS in patients not taking GABA agonists as compared to patients taking GABA agonists
Zhang et al. 2019 (Zhang et al., 2019)	AD	15 (real) 13 (sham)	69.00±8.19 68.54±7.93	rTMS (10 Hz) 2000 pulses 20 sessions	100% rMT	l DLPFC l LTL	3T	PRESS	8	1500/35	10 × 10 × 20	l DLPFC l LTL	Greater DLPFC NAA/Cr change after real rTMS as compared to sham Greater DLPFC Cho/Cr change after sham rTMS as compared to real Greater DLPFC mIns/Cr change after sham rTMS as compared to real Neg. correlation between DLPFC NAA/Cr change and cognitive score change after real rTMS

2DJ:2-dimensional J-resolved, AD: Alzheimer's disease, aud.: auditory, bil.: bilateral, dom.: dominant, GM: grey matter, hipp.: hippocampus, MC: motor cortex, PD: Parkinson's disease, temp.: temporal, TRD: treatment-resistant depression, S2: secondary somatosensory cortex, SZ: schizophrenia, WM: white matter, WSCT: Wisconsin Card Sorting Test.

2015), NAA/Cr in the left DLPFC (Erbay et al., 2019), Cho in the left DLPFC (Luborzewski et al., 2007) and MI levels in the left PFC (Zheng et al., 2010) increased after rTMS treatment. Furthermore, the increase of NAA in the left ACC (Zheng et al., 2015) and MI levels in the left PFC (Zheng et al., 2010) were associated with improved cognitive performance and reduction of symptom severity as measured by the HAMD.

2.2.3.2. Other pathological conditions. In contrast to the amount of rTMS-MRS literature available in patients with depression, rTMS interventions combined with MRS as a readout in other pathological conditions are, so far, limited to single studies. The main findings of these studies are discussed below. An overview of the studies and more detailed study parameters are presented in Table 4A.

In dystonia patients and healthy controls, the effect of two rTMS sessions (separated in time) on GABA, Glx and NAA levels in both M1s, both lentiform nuclei and the occipital cortex was evaluated (Marjanska et al., 2013). Baseline metabolite levels did not differ between groups. After the intervention, NAA and Glx levels in the dominant M1 decreased similarly in both groups. Interestingly, GABA levels in the dominant M1 were modulated differently. While GABA levels decreased in patients with dystonia, an increase was reported in healthy controls. rTMS induced changes in metabolite levels were interpreted in terms of an increased energy demand induced by rTMS. The opposite GABA modulation patterns observed between groups might be explained by differences in processes of GABA synthesis (Marjanska et al., 2013).

In patients with ALS, GABA and glutamate levels in the left M1 and glutamate levels in the left white matter caudally to M1 and in the tegmen of the pons were not altered after bilateral cTBS applied over M1 (Di Lazzaro et al., 2017). Nonetheless, a positive relationship was observed between an rTMS-induced enhancement in M1 GABA levels and reduced disease progression.

Another study evaluated the effect of iTBS on cortical excitability, glutamate and other key metabolites [Gln, glucose (Glc), MI, NAA, GSH, Cho and Cr] in the left M1 in subjects with diabetes (type-2 diabetes mellitus), pre-diabetes and healthy controls (Fried et al., 2019). The results of this study showed that (1) metabolite levels (Gln/tCr, Gln/Glu, Glc/tCr and Cho/tCr) differed between groups, (2) no overall modulatory effect of iTBS on cortical excitability, measured with spTMS and (3) a positive relationship between an iTBS-enhanced MEP amplitude and increased Glu/tCr ratio in subjects with diabetes, but not in the other groups. These results highlight that cortical plasticity is impaired in subjects with diabetes and prediabetes as compared to healthy controls, and that for subjects with diabetes, neuroplastic mechanisms can be linked with glutamate levels in M1 (Fried et al., 2019).

In a sham-controlled study including patients with Alzheimer's Disease, the effect of a long-term rTMS intervention (20 sessions, 5 sessions/week) coupled with cognitive training on cognitive, behavioral and metabolic outcome parameters was evaluated (Zhang et al., 2019). In each session, rTMS was first applied for 10 min over left DLPFC, followed by 10 min of stimulation over the left lateral temporal lobe (LTL). Patients who received real rTMS showed increased behavioral and cognitive improvements and an elevated NAA/Cr ratio in the left DLPFC as compared to patients in the sham condition. Furthermore, a positive relationship between the change in NAA/Cr ratio in the left DLPFC and change in cognitive performance emerged after the intervention. Moreover, an increase in NAA/Cr ratio was associated with better cognitive performance.

In a double-blind randomized control trial, schizophrenia patients underwent a 30-session treatment with either real rTMS or sham (10 sessions/week, 2 per day). rTMS (or sham) was administered over left DLPFC in the morning session and over the right DLPFC in the afternoon session (Dlabac-de Lange et al., 2017). Changes in Glx and NAA levels in the left DLPFC were measured before and after treatment. Results indicated an increase of Glx levels after real rTMS and a decrease after sham, while NAA levels did not change.

Two patient studies identified the effect of multiple sessions of rTMS over the right DLPFC. The first study evaluated metabolic changes (NAA, Cho and Cr) in the left and right hippocampus following real high-frequency rTMS or sham in a group of detoxified alcohol-dependent patients (Qiao et al., 2016). Real rTMS (as compared to sham) resulted in a higher increase in NAA/Cr and Cho/Cr ratios and this increase was associated with improved memory performance. The second study described a single case of a patient that was treated with low-frequency rTMS for a combination of substance use, anxiety and depression (Hone-Blanchet et al., 2017). After treatment, the patient showed substantial clinical improvement, and this was paralleled by metabolic changes. More specifically, Glx levels increased in the right DLPFC, right striatum and right ACC. NAA increased in right DLPFC and striatum, but not in ACC. In contrast, GABA levels did not change after rTMS.

A sham-controlled clinical trial evaluated the effect of rTMS (10 sessions, 5 sessions/week) over the right secondary somatosensory cortex on metabolite levels (NAA, Cho, Glu, Gln, mIns and Cr) and clinical parameters in patients with chronic visceral pain (Fregni et al., 2011). After real rTMS (but not after sham), NAA and glutamate levels increased in the left and right secondary somatosensory cortex. Moreover, increased NAA and glutamate levels were associated with significant pain reduction, which lasted for at least 3 weeks after treatment.

In tinnitus patients, a prospective randomized single-blind sham-controlled crossover design evaluated the effect of rTMS (over 5 consecutive days) applied over the auditory cortex of the left temporal lobe on the loudness of tinnitus perception (Cacace et al., 2017). In parallel, rTMS-induced metabolic (NAA, Cho and Glu) changes in left and right auditory cortical areas were assessed. Real rTMS (but not sham) reduced tinnitus loudness and glutamate levels in the left (but not right) auditory cortex. Furthermore, it was shown that reduced tinnitus loudness was highly correlated with decreased glutamate levels after rTMS treatment.

In late-stage Parkinson's patients, metabolic profile changes in the right pre-supplementary motor area (preSMA) (NAA, Cho and Cr) were investigated following administration of a single session of rTMS and sham over the right preSMA using a sham-controlled crossover design (Flamez et al., 2019). Although neither real rTMS nor sham altered the NAA/Cr ratio, real rTMS affected the Cho/Cr ratio, but only when disease duration was taken into account. More specific, shorter disease duration was associated with stronger rTMS-induced effects. This finding may suggest that brain plasticity is preserved, at least in the early part of the advanced stage of the disease (Flamez et al., 2019).

2.2.3.3. PAS. One study applied a PAS protocol in patients with MS and healthy controls (see Table 4A) (Zeller et al., 2010). More specific, electrical stimulation applied at the median nerve of the dominant hand was combined with spTMS over the contralateral M1. The NAA/Cr ratio in the corpus callosum and corticomuscular latency were assessed to evaluate central nervous system (CNS) injury. As expected, a lower NAA/Cr ratio and a higher corticomuscular latency were reported in patients as compared to healthy controls. It was also shown that PAS-enhanced cortical excitability and training-induced motor performance in a similar way in both groups. PAS-induced changes were not associated with the NAA/Cr ratio.

2.2.4. A TMS train as a tool to evaluate phosphene thresholds combined with MRS

In healthy controls and subjects with grapheme-color synesthesia, which is defined as a neurological condition characterized by an over-binding of different features and visual cortex hyperexcitability (Terhune et al., 2011), in which letters and numbers involuntary elicit color photisms (Rouw and Scholte, 2010), the relationship between TMS-induced phosphenes and baseline GABA and glutamate levels in the occipital cortex and left M1 was investigated (see Table 4B) (Terhune et al., 2015). This study indicated that TMS-induced phosphene thresholds were negatively associated with local

Table 4B
Overview of studies combining MRS with TMS as a tool to evaluate phosphene thresholds in patient populations.

Study	Demographics			TMS			MRS						Significant findings TMS-MRS relation
	Population	N	Age	Protocol	Intensity	Region	FS	Sequence	Averages	TR/TE (ms)	Voxel size (mm^3)	Region	
Terhune et al. 2015 (Terhune et al., 2015)	Grapheme-color synesthesia ctrl	11	22.3 ± 1.1 23.01±1.6	rTMS 1 session	adjustable	V1	3T	SPECIAL	128	4000/8.5	20 × 20 × 20	OCC l M1	Neg. correlation between visual cortex Glu/Cr and phosphene threshold in total sample, synesthetes and controls

glutamate levels in the primary visual cortex. Additionally, it was reported that these metrics covaried with the visuospatial phenomenology of grapheme-color synesthesia (Terhune et al., 2015).

2.3. Summary of findings

Given the variability in the applied MRS and TMS methodologies, the diversity of patient populations, and contradictory and/or unreplicated findings, caution is needed when interpreting the results of the reviewed studies.

In general, an association between TMS and MRS measures has not been consistently found in studies in healthy individuals investigating $GABA_A$-mediated inhibition, suggesting that TMS and MRS probably do not measure similar features of the GABAergic system, but rather complementary features. GABA levels measured with MRS are assumed to be associated with tonic and not phasic inhibition and may therefore not reflect synaptic activity. No association between $GABA_B$-mediated inhibition and MRS-GABA levels has been found either, however, several studies suggest an association between Glx or glutamate and TMS measures. At this point, there are too few studies in patient populations to draw any conclusions regarding the association between TMS and MRS measures in disease.

TMS has mainly been used as an intervention in patients with depression and it appears that TMS induces changes in prefrontal glutamatergic and GABAergic levels. However, the strength and direction of these changes may depend on responsiveness to interventional TMS as defined by a reduction of depressive symptoms. Interventional TMS combined with MRS measures in other diseases is thus far limited to single studies. A few studies combining interventional TMS and MRS measures in healthy individuals suggest an association between TMS-induced GABA and/or Glx changes and functional connectivity strength.

Although the majority of studies have been focusing on GABA and Glx, a limited number of studies in humans indicated that neurotransmitters such as dopamine and serotonin could also be modulated by rTMS. For example, in patients with major depression, rTMS applied over prefrontal brain regions, was shown to release dopamine in striatal regions (Pogarell et al., 2007; Pogarell et al., 2006) and to restore the serotonergic system as indicated by a serotonin 5-hydroxytryptamine$_{2A}$-receptor upregulation in the DLPFC and a downregulation in the hippocampus (Baeken et al., 2011). Another study, investigating the pain modulating effects of rTMS applied over the right primary motor/sensory area, suggested that analgesic rTMS effects are likely mediated via a cascade of activation of the striatal dopamine and opioid systems (Lamusuo et al., 2017).

3. Limitations

3.1. TMS

A first limitation is that most TMS protocols identified M1 related measures of excitability and or receptor-mediated inhibition and facilitation in the human motor system. The application of a TEP protocol might offer an alternative approach revealing not only information in the vicinity of the stimulation location, but also in remote interconnected brain regions (Bonato et al., 2006; Ilmoniemi et al., 1997; Lioumis et al., 2009).

A second limitation is that only a limited amount of TMS protocols are available to measure metabolic-related physiological processes, including metrics of $GABA_A$, $GABA_B$ and glutamate receptor-mediated neurotransmission. In contrast, MRS has the advantage that the chemical shift spectrum contains information about the concentration of a broad range of metabolites, including GABA and glutamate, but also other metabolites such as described earlier.

A third limitation relates to the variability inherent to TMS measurements. In this respect, several studies formulated recommendations in terms of the number of pulses needed to achieve reliable estimates of TMS outcomes (Cuypers et al., 2014; Chang et al., 2016; Goldsworthy et al., 2016). Overall, 20–30 pulses per condition seem to be sufficient, depending on the paradigm (spTMS vs. ppTMS) and whether a neuronavigational system is used. When employing a neuronavigational system the number of pulses can be reduced up to 30% (Chang et al., 2016). Also, the reliability of TMS parameters on the subject level (but not on the group level) can be reduced when controlling the accuracy of the coil positioning (de Goede et al., 2018). For ppTMS paradigms, expressing the intensity of the conditioning stimulus as a percentage of the individual threshold for intracortical facilitation or inhibition will reduce the variability of ppTMS measurements (Orth et al., 2003).

A fourth limitation is related to the assessment of TEPs, whereby overcoming artifacts in EEG signals induced by TMS constitutes a major limitation. Both the sound produced and current induced by TMS, evoke changes in brain activity signals. To overcome this limitation, inclusion of a realistic sham condition is essential to draw valid conclusions from TEP studies (Conde et al., 2019; Siebner et al., 2019).

A final limitation is that for rTMS interventions, it remains unclear which biomarkers successfully predict the response to the intervention. For example for depression, a review revealed that patient, illness and TMS procedure related factors play a role in predicting the outcome for rTMS were recently reviewed (Kar, 2019). However, to further improve predictions, future research overcoming differences in sample selection variations and small sample sizes is highly recommended. In this respect, the exploration of MRS-related biomarkers is desirable since pretreatment glutamate levels in the left DLPFC seem to be associated with the rTMS outcome (Luborzewski et al., 2007). More specifically, patients with lower glutamate levels appeared to respond better to the treatment.

3.2. MRS

Although ^{1}H-MRS is the only non-invasive method enabling direct, *in vivo* quantification of metabolite levels, particularly those of glutamate and GABA, it has several limitations. Firstly, the acquisition of brain ^{1}H-MR spectra of sufficient quality takes a considerable amount of time, particularly at lower clinical magnetic field strengths. Since only single-voxel MRS methods are currently widely available, ^{1}H-MRS studies are usually restricted to one or few brain regions. Furthermore, because of the low SNR of particularly glutamate and GABA, relatively large voxel sizes are commonly applied. Scan duration, size, positioning and exact anatomical location of MRS volumes, B_0 shimming and used MRS pulse sequence affect spectral quality and can differ between studies, which complicates comparisons across studies and might partially explain the inconsistencies between the reviewed studies. Single-voxel methods require preselection based on hypotheses and previous findings. Therefore, when using single-voxel approaches, metabolite changes in the largest part of the brain remain undetected. This limitation makes it difficult to prove the spatial specificity of metabolic changes and network effects. Additionally, MRS voxels cannot be placed too close to the skull because of the risk of lipid artefacts, which complicates the investigation of potential associations between TMS measures or interventional TMS on the one side and MRS measures on the other side. Furthermore, one cannot distinguish between intracellular and extracellular pools of metabolites from the information acquired with MRS.

Secondly, the relatively low signals of glutamate and GABA pose methodological challenges because of their overlap with signals from other metabolites. At lower clinical field strengths, where separation of the glutamate and glutamine signals is unreliable (De Graaf, 2019), these signals are commonly combined into one Glx signal. Assessment of the GABA signal is particularly challenging because of its overlap with the more abundant creatine resonance and MM resonances. Detection of the GABA signal is therefore not possible using conventional ^{1}H-MRS sequences and requires J-difference edited, DQF or 2D-MRS, of which the first is the most commonly used approach because of the wide availability of pulse sequences and analysis tools. However, ac-

quisition of the isolated GABA signal requires even longer scan times and/or larger voxels as compared to conventional ^{1}H-MRS. Moreover, acquisition of the MM-uncontaminated GABA signal is challenging at clinical field strengths and the use of MM-unsuppressed GABA-editing techniques may complicate the interpretation of findings (Harris et al., 2015). Improved accuracy of MRS measurements is observed at higher field strengths and shorter TEs with very good reliability at 3T for the major spectral components (Oz et al., 2014), while the sensitivity and resolution of 7T are beneficial for weak signals, short acquisition times and small volumes (Terpstra et al., 2016). Edited MRS at 3T shows reliable measurement of GABA with higher precision as compared to non-edited and 2D approaches (Baeshen et al., 2020). At 7T, high accuracy and reproducibility of glutamate and (edited) GABA are observed, with test-retest concentration differences being smaller than concentration differences between subjects (Prinsen et al., 2017).

Thirdly, precise estimation of metabolite concentrations from ^{1}H-MR spectra is difficult. Many studies use creatine as a reference to normalize metabolite levels, whereas NAA and choline are used as a reference to a lesser extent. However, creatine, NAA and choline may change in disease and during normal ageing (Maddock and Buonocore, 2012; De Graaf, 2019; Moffett et al., 2007; Holmes et al., 2017; Levin et al., 2019; Marsman et al., 2013; Maudsley et al., 2012; Reyngoudt et al., 2012; Suri et al., 2017; Cichocka and Beres, 2018). Using the water signal as a reference appears to be a more reliable method (Gasparovic et al., 2006), although the brain water concentration may also change in certain conditions (Jansen et al., 2006; Grasso et al., 2002; Laule et al., 2004). Several caveats must be considered when using the water signal as an internal reference, as the accuracy of the method relies on estimates of fractional tissue water, estimates of water relaxation times and accuracy of the segmentation method used to measure tissue fractions in the MRS voxel (Gasparovic et al., 2006).

Lastly, in simultaneous TMS-MRS designs, it is important to take into account the BOLD effect induced by TMS (Bestmann et al., 2005; Bohning et al., 2000). The BOLD effect may influence spectral linewidth and appropriate linewidth correction may thus be necessary when TMS and MRS are concurrently performed (Bednarik et al., 2015; Mangia et al., 2006; Schaller et al., 2013; Schaller et al., 2014; Stanley and Raz, 2018; Zhu and Chen, 2001; Mangia et al., 2007), however, to the best of our knowledge, this has not been applied so far. Furthermore, TMS may induce changes in tissue volume fractions in the MRS voxel due to changes in cerebral blood flow and volume affecting CSF volume and vascular space occupancy (Jin and Kim, 2010; Lu et al., 2003). To overcome this issue, the total creatine, NAA or choline signal could be used as an internal reference to normalize metabolite levels, provided that the reference metabolite concentration is not subject to any changes during the experiment or study.

Overall, interpretation of MRS data is complicated by the biochemical role of the metabolites. Most metabolites are involved in multiple biochemical pathways and altered concentrations should be interpreted in the light of the context of the study, taking into consideration that there are still gaps in the knowledge about the biochemical roles of MRS detectable metabolites (Rae, 2014).

4. Future perspectives

By combining TMS with EEG, the functionality of glutamatergic and GABA receptor-mediated neurotransmission can be explored within and especially beyond M1. In contrast, MEPs resulting from conventional TMS paradigms (combined with EMG alone) yield only information concerning M1. Furthermore, the advantage of combining both modalities is that they can provide a more complete picture of metabolite levels (MRS) and high-resolution receptor-mediated modulation of neurotransmitter systems (TEP) in brain regions beyond M1.

Another promising development is multi-locus TMS (mTMS) (Koponen et al., 2018). This technique allows multiple coils (embedded in a single coil former) to change its stimulation spots electronically, without movement of the coil itself. Recently, this technique was used to evaluate to which extent SICI can be influenced by varying the timing and the location of the CS with respect to the TS applied over M1 (Nieminen et al., 2019). The results provide new evidence supporting the view that inhibition at ISI's of 0.5 and 2.5 ms is mediated by distinct mechanisms or neuronal elements. However, more experiments are needed to ascertain the contribution of this technique for improving our understanding of receptor-mediated modulation of inhibition or facilitation. Besides new possibilities for neurostimulation, it is expected that mTMS will also be used for neuromodulation (Ziemann et al., 2019). Moreover, the goal is to develop a subject-specific closed-loop (registering and altering brain activity) stimulation approach, targeting suboptimal or impaired cortical networks. Nonetheless, the future will reveal what the impact of this innovative technique will be, compared to the more conventional rTMS treatment protocols, and what the efficiency of this approach is regarding the restoration of altered metabolic levels in the patient's brain.

As ^{1}H-MRS is currently predominantly acquired during rest and thus used as a static measure, functional MRS (fMRS) holds promise for use in studies concurrently applying MRS and TMS. Current fMRS approaches allow tracking modulations in brain metabolite levels at a time scale of under a minute during brain stimulation by e.g. a cognitive task or TMS (Stanley and Raz, 2018). Technological developments at higher magnetic field strengths are particularly beneficial for dynamic detection of glutamate and GABA and concurrent TMS-fMRS studies may therefore shed new light on the interplay between glutamate and GABA levels in the brain on the one side and neuromodulation and neurostimulation on the other side.

^{31}P-MRS may provide a valuable tool in addition to ^{1}H-MRS to probe cellular energetics and potential changes in energy demand during or after TMS. With ^{31}P-MRS it is possible to detect compounds of energy metabolism such as ATP, PCr and inorganic phosphate (P_i), and cell membrane phospholipid precursors (phosphomonoesters, PME) and breakdown products (phosphodiesters, PDE). Using saturation transfer experiments, the high-energy phosphate exchange between ATP and PCr and between ATP and P_i can be determined (Chen et al., 2018; Chen et al., 1997; Cady, 2012). Brain activation also evokes changes in acidity, which can be derived using the pH sensitive resonance position of the P_i signal (Hendriks et al., 2019).

5. Conclusion

This review summarizes techniques and measures that are commonly used when combining TMS and MRS. Combined TMS-MRS studies provide a sensitive tool for investigation of the healthy and diseased brain, as the two techniques reveal complementary and comprehensive information on brain metabolism, in particular GABAergic and glutamatergic neurotransmission. The combination of TMS and MRS can be used to evaluate alterations of metabolite levels following interventional TMS, as well as identify the interplay between brain metabolism and excitation, inhibition or facilitation. Potentially, connectivity changes and dedicated network interactions can be probed using the combined TMS-MRS approach. Considering the ongoing technical developments in the fields of TMS and MRS, combined studies hold future promise for more precise investigations of brain network interactions, neurotransmission and energetics.

CRediT authorship contribution statement

Koen Cuypers: Conceptualization, Methodology, Validation, Formal analysis, Investigation, Resources, Writing - original draft, Writing - review & editing, Visualization. **Anouk Marsman:** Conceptualization, Methodology, Validation, Formal analysis, Investigation, Resources, Writing - original draft, Writing - review & editing, Visualization.

Acknowledgment

We would like to thank Prof. Stephan Swinnen and Dr. Axel Thielscher for a critical reading of the manuscript.

Funding sources

This work was supported by the KU Leuven Special Research Fund grant (C16/15/070), Research Foundation Flanders grant (G089818N), and the Excellence of Science grant (EOS 30446199, MEMODYN).

References

Allen, C.P., et al., 2014. Enhanced awareness followed reversible inhibition of human visual cortex: a combined TMS, MRS and MEG study. PLoS One 9 (6), e100350.
Amunts, K., et al., 1996. Asymmetry in the human motor cortex and handedness. Neuroimage 4 (3 Pt 1), 216–222.
Arun, P., et al., 2006. Regulation of N-acetylaspartate and N-acetylaspartylglutamate biosynthesis by protein kinase activators. J. Neurochem. 98 (6), 2034–2042.
Baeken, C., et al., 2011. The impact of HF-rTMS treatment on serotonin(2A) receptors in unipolar melancholic depression. Brain Stimul 4 (2), 104–111.
Baeken, C., Lefaucheur, J.P., Van Schuerbeek, P., 2017. The impact of accelerated high frequency rTMS on brain neurochemicals in treatment-resistant depression: insights from (1)H MR spectroscopy. Clin. Neurophysiol. 128 (9), 1664–1672.
Baeshen, A., et al., 2020. Test-Retest Reliability of the Brain Metabolites GABA and Glx With JPRESS, PRESS, and MEGA-PRESS MRS Sequences *in vivo* at 3T. J. Magn. Reson. Imaging 51 (4), 1181–1191.
Bak, L.K., Schousboe, A., Waagepetersen, H.S., 2006. The glutamate/GABA-glutamine cycle: aspects of transport, neurotransmitter homeostasis and ammonia transfer. J. Neurochem. 98 (3), 641–653.
Bednarik, P., et al., 2015. Neurochemical and BOLD responses during neuronal activation measured in the human visual cortex at 7 Tesla. J. Cereb. Blood Flow Metab. 35 (4), 601–610.
Belardinelli, P., et al., 2019. Reproducibility in TMS-EEG studies: a call for data sharing, standard procedures and effective experimental control. Brain Stimul. 12 (3), 787–790.
Bestmann, S., et al., 2005. BOLD MRI responses to repetitive TMS over human dorsal premotor cortex. Neuroimage 28 (1), 22–29.
Bhogal, A.A., et al., 2017. (1) H-MRS processing parameters affect metabolite quantification: the urgent need for uniform and transparent standardization. NMR Biomed. 30 (11).
Boer, V.O., et al., 2015. Parallel reconstruction in accelerated multivoxel MR spectroscopy. Magn. Reson. Med. 74 (3), 599–606.
Bogner, W., et al., 2017. 1D-spectral editing and 2D multispectral *in vivo*(1)H-MRS and (1)H-MRSI - Methods and applications. Anal. Biochem. 529, 48–64.
Bohning, D.E., et al., 2000. BOLD-f MRI response to single-pulse transcranial magnetic stimulation (TMS). J. Magn. Reson. Imaging 11 (6), 569–574.
Bonato, C., Miniussi, C., Rossini, P.M., 2006. Transcranial magnetic stimulation and cortical evoked potentials: a TMS/EEG co-registration study. Clin. Neurophysiol. 117 (8), 1699–1707.
Bridges, N.R., et al., 2018. Single session low frequency left dorsolateral prefrontal transcranial magnetic stimulation changes neurometabolite relationships in healthy humans. Front. Hum. Neurosci. 12, 77.
Buonocore, M.H., Maddock, R.J., 2015. Magnetic resonance spectroscopy of the brain: a review of physical principles and technical methods. Rev. Neurosci. 26 (6), 609–632.
Cacace, A.T., et al., 2017. Glutamate is down-regulated and tinnitus loudness-levels decreased following rTMS over auditory cortex of the left hemisphere: a prospective randomized single-blinded sham-controlled cross-over study. Hear. Res. 358, 59–73.
Cady, E.B., 2012. In vivo cerebral 31P magnetic resonance spectroscopy. In: Choi, L.Y., Gruetter, R. (Eds.), Neural Metabolism in Vivo. Springer, New York, pp. 149–180.
Cangro, C.B., et al., 1987. Immunohistochemistry and biosynthesis of N-acetylaspartylglutamate in spinal sensory ganglia. J. Neurochem. 49 (5), 1579–1588.
Carson, R.G., et al., 2013. Characterizing changes in the excitability of corticospinal projections to proximal muscles of the upper limb. Brain Stimul. 6 (5), 760–768.
Cash, R.F., et al., 2017. Characterization of Glutamatergic and GABAA-mediated neurotransmission in motor and dorsolateral prefrontal cortex using paired-pulse TMS-EEG. Neuropsychopharmacology 42 (2), 502–511.
Chang, W.H., et al., 2016. Optimal number of pulses as outcome measures of neuronavigated transcranial magnetic stimulation. Clin. Neurophysiol. 127 (8), 2892–2897.
Chen, R., et al., 1997a. Depression of motor cortex excitability by low-frequency transcranial magnetic stimulation. Neurology 48 (5), 1398–1403.
Chen, W., et al., 1997b. Increase of creatine kinase activity in the visual cortex of human brain during visual stimulation: a 31P magnetization transfer study. Magn. Reson. Med. 38 (4), 551–557.
Chen, R., et al., 1998. Intracortical inhibition and facilitation in different representations of the human motor cortex. J. Neurophysiol. 80 (6), 2870–2881.
Chen, R., et al., 2008. The clinical diagnostic utility of transcranial magnetic stimulation: report of an IFCN committee. Clin. Neurophysiol. 119 (3), 504–532.
Chen, C., et al., 2018. (31) P magnetization transfer magnetic resonance spectroscopy: assessing the activation induced change in cerebral ATP metabolic rates at 3 T. Magn. Reson. Med. 79 (1), 22–30.
Chen, R., 2000. Studies of human motor physiology with transcranial magnetic stimulation. Muscle Nerve Suppl. 9, S26–S32.
Cichocka, M., Beres, A., 2018. From fetus to older age: a review of brain metabolic changes across the lifespan. Ageing Res. Rev. 46, 60–73.
Classen, J., et al., 2004. Paired associative stimulation. Suppl. Clin. Neurophysiol. 57, 563–569.
Cleeland, C., et al., 2019. Neurochemical changes in the aging brain: a systematic review. Neurosci. Biobehav. Rev. 98, 306–319.
Conde, V., et al., The non-transcranial TMS-evoked potential is an inherent source of ambiguity in TMS-EEG studies. Neuroimage, 2019.185: p. 300–312.
Croarkin, P.E., et al., 2016. Transcranial magnetic stimulation potentiates glutamatergic neurotransmission in depressed adolescents. Psychiatry Res Neuroimaging 247, 25–33.
Cuypers, K., Thijs, H., Meesen, R.L., 2014. Optimization of the transcranial magnetic stimulation protocol by defining a reliable estimate for corticospinal excitability. PLoS One 9 (1), e86380.
Cuypers, K., et al., 2020. Task-related measures of short-interval intracortical inhibition and GABA levels in healthy young and older adults: a multimodal TMS-MRS study. Neuroimage 208, 116470.
Darmani, G., Ziemann, U., 2019. Pharmacophysiology of TMS-evoked EEG potentials: a mini-review. Brain Stimul 12 (3), 829–831.
Daskalakis, Z.J., et al., 2008. Long-interval cortical inhibition from the dorsolateral prefrontal cortex: a TMS-EEG study. Neuropsychopharmacology 33 (12), 2860–2869.
de Goede, A.A., Ter Braack, E.M., van Putten, M., 2018. Accurate Coil Positioning is Important for Single and Paired Pulse TMS on the Subject Level. Brain Topogr. 31 (6), 917–930.
De Graaf, R.A., 2019a. In Vivo NMR spectroscopy: Principles and Techniques. Wiley.
De Graaf, R.A., 2019b. In vivo NMR spectroscopy - static aspects. In: Proceedings of the In Vivo NMR Spectroscopy: Principles and Techniques, pp. 43–128.
De Graaf, R.A., 2019c. Spectral editing and 2D NMR. In: Proceedings of the In Vivo NMR Spectroscopy: Principles and Techniques, pp. 375–438.
Devanne, H., Lavoie, B.A., Capaday, C., 1997. Input-output properties and gain changes in the human corticospinal pathway. Exp. Brain Res. 114 (2), 329–338.
Di Lazzaro, V., et al., 2000. Direct demonstration of the effect of lorazepam on the excitability of the human motor cortex. Clin. Neurophysiol. 111 (5), 794–799.
Di Lazzaro, V., et al., 2017. Effects of repetitive TMS of the motor cortex on disease progression and on glutamate and GABA levels in ALS: a proof of principle study. Brain Stimul 10 (5), 1003–1005.
Ding, X.Q., Lanfermann, H., 2015. Whole brain (1)H-Spectroscopy: a developing technique for advanced analysis of cerebral metabolism. Clin. Neuroradiol. 25 (Suppl 2), 245–250.
Dlabac-de Lange, J.J., et al., 2017. Effect of bilateral prefrontal rTMS on left prefrontal NAA and Glx levels in schizophrenia patients with predominant negative symptoms: an exploratory study. Brain Stimul. 10 (1), 59–64.
Du, X., et al., 2018a. TMS evoked N100 reflects local GABA and glutamate balance. Brain Stimul. 11 (5), 1071–1079.
Du, X., et al., 2018b. Cerebellar-stimulation evoked prefrontal electrical synchrony is modulated by GABA. Cerebellum 17 (5), 550–563.
Dubin, M.J., et al., 2016. Elevated prefrontal cortex GABA in patients with major depressive disorder after TMS treatment measured with proton magnetic resonance spectroscopy. J. Psychiatry Neurosci. 41 (3), E37–E45.
Dyke, K., et al., 2017. Comparing GABA-dependent physiological measures of inhibition with proton magnetic resonance spectroscopy measurement of GABA using ultra-high-field MRI. Neuroimage 152, 360–370.
Edden, R.A., Pomper, M.G., Barker, P.B., 2007. In vivo differentiation of N-acetyl aspartyl glutamate from N-acetyl aspartate at 3 Tesla. Magn. Reson. Med. 57 (6), 977–982.
Edden, R.A., et al., 2014. Gannet: a batch-processing tool for the quantitative analysis of gamma-aminobutyric acid-edited MR spectroscopy spectra. J. Magn. Reson. Imaging 40 (6), 1445–1452.
Erbay, M.F., et al., 2019. Evaluation of transcranial magnetic stimulation efficiency in major depressive disorder patients: a magnetic resonance spectroscopy study. Psychiatry Investig.
Erecinska, M., Silver, I.A., 1989. ATP and brain function. J. Cereb. Blood Flow Metab. 9 (1), 2–19.
Farzan, F., et al., 2010. Reliability of long-interval cortical inhibition in healthy human subjects: a TMS-EEG study. J. Neurophysiol. 104 (3), 1339–1346.
Ferreri, F., et al., 2011. Human brain connectivity during single and paired pulse transcranial magnetic stimulation. Neuroimage 54 (1), 90–102.
Fisher, R.J., et al., 2002. Two phases of intracortical inhibition revealed by transcranial magnetic threshold tracking. Exp. Brain Res. 143 (2), 240–248.
Flamez, A., et al., 2019. The influence of one session of low frequency rTMS on pre-supplementary motor area metabolites in late stage Parkinson's disease. Clin. Neurophysiol. 130 (8), 1292–1298.
Frahm, J., et al., 1996. Dynamic uncoupling and recoupling of perfusion and oxidative metabolism during focal brain activation in man. Magn. Reson. Med. 35 (2), 143–148.
Fregni, F., et al., 2011. Clinical effects and brain metabolic correlates in non-invasive cortical neuromodulation for visceral pain. Eur. J. Pain 15 (1), 53–60.
Fried, P.J., Pascual-Leone, A., Bolo, N.R., 2019. Diabetes and the link between neuroplasticity and glutamate in the aging human motor cortex. Clin. Neurophysiol. 130 (9), 1502–1510.
Gabbay, V., et al., 2007. Lateralized caudate metabolic abnormalities in adolescent major depressive disorder: a proton MR spectroscopy study. Am. J. Psychiatry 164 (12), 1881–1889.
Gasparovic, C., et al., 2006. Use of tissue water as a concentration reference for proton spectroscopic imaging. Magn. Reson. Med. 55 (6), 1219–1226.

Gehl, L.M., et al., 2004. Biosynthesis of NAAG by an enzyme-mediated process in rat central nervous system neurons and glia. J. Neurochem. 90 (4), 989–997.
Goldsworthy, M.R., Hordacre, B., Ridding, M.C., 2016. Minimum number of trials required for within- and between-session reliability of TMS measures of corticospinal excitability. Neuroscience 320, 205–209.
Govind, V., Young, K., Maudsley, A.A., 2000. Corrigendum: proton NMR chemical shifts and coupling constants for brain metabolites. NMR Biomed 13, 129–153 NMR Biomed, 2015.**28**(7): p. 923-4.
Govindaraju, V., Young, K., Maudsley, A.A., 2000. Proton NMR chemical shifts and coupling constants for brain metabolites. NMR Biomed. 13 (3), 129–153.
Grasso, G., et al., 2002. Assessment of human brain water content by cerebral bioelectrical impedance analysis: a new technique and its application to cerebral pathological conditions. Neurosurgery 50 (5), 1064–1072 discussion 1072-4.
Greenhouse, I., et al., 2017. Individual differences in resting corticospinal excitability are correlated with reaction time and GABA content in motor cortex. J. Neurosci. 37 (10), 2686–2696.
Grohn, H., et al., 2019. Influence of Repetitive Transcranial Magnetic Stimulation on Human Neurochemistry and Functional Connectivity: a Pilot MRI/MRS Study at 7 T. Front Neurosci 13, 1260.
Harris, A.D., et al., 2015. Spectral-editing measurements of GABA in the human brain with and without macromolecule suppression. Magn. Reson. Med. 74 (6), 1523–1529.
Hendriks, A.D., et al., 2019. SNR optimized (31) P functional MRS to detect mitochondrial and extracellular pH change during visual stimulation. NMR Biomed. 32 (11), e4137.
Hermans, L., et al., 2018. GABA levels and measures of intracortical and interhemispheric excitability in healthy young and older adults: an MRS-TMS study. Neurobiol. Aging 65, 168–177.
Hofmann, L., et al., 2002. Quantitative 1H-magnetic resonance spectroscopy of human brain: influence of composition and parameterization of the basis set in linear combination model-fitting. Magn. Reson. Med. 48 (3), 440–453.
Holmes, M.J., et al., 2017. Longitudinal increases of brain metabolite levels in 5-10 year old children. PLoS One 12 (7), e0180973.
Hone-Blanchet, A., et al., 2015. Co-registration of magnetic resonance spectroscopy and transcranial magnetic stimulation. J. Neurosci. Methods 242, 52–57.
Hone-Blanchet, A., Mondino, M., Fecteau, S., 2017. Repetitive transcranial magnetic stimulation reduces anxiety symptoms, drug cravings, and elevates (1)H-MRS brain metabolites: a case report. Brain Stimul 10 (4), 856–858.
Hong, D., et al., 2019. A comparison of sLASER and MEGA-sLASER using simultaneous interleaved acquisition for measuring GABA in the human brain at 7T. PLoS One 14 (10), e0223702.
Huang, Y.Z., et al., 2005. Theta burst stimulation of the human motor cortex. Neuron 45 (2), 201–206.
Ilmoniemi, R.J., Kicic, D., 2010. Methodology for combined TMS and EEG. Brain Topogr. 22 (4), 233–248.
Ilmoniemi, R.J., et al., 1997. Neuronal responses to magnetic stimulation reveal cortical reactivity and connectivity. Neuroreport 8 (16), 3537–3540.
Lioumis, P., et al., 2009. Reproducibility of TMS-Evoked EEG responses. Hum. Brain Mapp. 30 (4), 1387–1396.
Inghilleri, M., et al., 1993. Silent period evoked by transcranial stimulation of the human cortex and cervicomedullary junction. J. Physiol. 466, 521–534.
Irlbacher, K., et al., 2007. Effects of GABA(A) and GABA(B) agonists on interhemispheric inhibition in man. Clin. Neurophysiol. 118 (2), 308–316.
Iwabuchi, S.J., et al., 2017. Targeted transcranial theta-burst stimulation alters fronto-insular network and prefrontal GABA. Neuroimage 146, 395–403.
Jannati, A., et al., 2019. Test-retest reliability of the effects of continuous theta-burst stimulation. Front. Neurosci. 13, 447.
Jansen, J.F., et al., 2006. 1H MR spectroscopy of the brain: absolute quantification of metabolites. Radiology 240 (2), 318–332.
Jin, T., Kim, S.G., 2010. Change of the cerebrospinal fluid volume during brain activation investigated by T(1rho)-weighted fMRI. Neuroimage 51 (4), 1378–1383.
Kantamneni, S., 2015. Cross-talk and regulation between glutamate and GABAB receptors. Front Cell Neurosci 9, 135.
Kar, S.K., 2019. Predictors of response to repetitive transcranial magnetic stimulation in depression: a review of recent updates. Clin. Psychopharmacol. Neurosci. 17 (1), 25–33.
Kaufmann, P., et al., 2004. Objective tests for upper motor neuron involvement in amyotrophic lateral sclerosis (ALS). Neurology 62 (10), 1753–1757.
Ke, Y., et al., 2000. Assessment of GABA concentration in human brain using two-dimensional proton magnetic resonance spectroscopy. Psychiatry Res. 100 (3), 169–178.
Keltner, J.R., et al., 1997. In vivo detection of GABA in human brain using a localized double-quantum filter technique. Magn. Reson. Med. 37 (3), 366–371.
Klomjai, W., Katz, R., Lackmy-Vallee, A., 2015. Basic principles of transcranial magnetic stimulation (TMS) and repetitive TMS (rTMS). Ann. Phys. Rehabil. Med. 58 (4), 208–213.
Koponen, L.M., Nieminen, J.O., Ilmoniemi, R.J., 2018. Multi-locus transcranial magnetic stimulation-theory and implementation. Brain Stimul. 11 (4), 849–855.
Kouchtir-Devanne, N., et al., 2012. Task-dependent changes of motor cortical network excitability during precision grip compared to isolated finger contraction. J. Neurophysiol. 107 (5), 1522–1529.
Kreis, R., 2004. Issues of spectral quality in clinical 1H-magnetic resonance spectroscopy and a gallery of artifacts. NMR Biomed. 17 (6), 361–381.
Kreis, R., 2016. The trouble with quality filtering based on relative Cramer–Rao lower bounds. Magn. Reson. Med. 75 (1), 15–18.
Kujirai, T., et al., 1993. Corticocortical inhibition in human motor cortex. J. Physiol. 471, 501–519.
Kukke, S.N., et al., 2014. Efficient and reliable characterization of the corticospinal system using transcranial magnetic stimulation. J. Clin. Neurophysiol. 31 (3), 246–252.
König, F., Belardinelli, P., Liang, C., Desideri, D., Müller-Dahlhaus, F., Caldana Gordon, P., Zipser, C., Zrenner, C., Ziemann, U., 2019. TMS-EEG signatures of glutamatergic neurotransmission in human cortex. biorXiv doi:10.1101/555920.
Lamusuo, S., et al., 2017. Neurotransmitters behind pain relief with transcranial magnetic stimulation - positron emission tomography evidence for release of endogenous opioids. Eur. J. Pain 21 (9), 1505–1515.
Laule, C., et al., 2004. Water content and myelin water fraction in multiple sclerosis. A T2 relaxation study. J. Neurol. 251 (3), 284–293.
Levin, O., et al., 2019. Sensorimotor cortex neurometabolite levels as correlate of motor performance in normal aging: evidence from a (1)H-MRS study. Neuroimage 202, 116050.
Levitt, J.G., et al., 2019. Dorsolateral prefrontal gamma-aminobutyric acid in patients with treatment-resistant depression after transcranial magnetic stimulation measured with magnetic resonance spectroscopy. J. Psychiatry Neurosci. 44 (4), 1–9.
Lewis, C.P., et al., 2016. An exploratory study of spectroscopic glutamatergic correlates of cortical excitability in depressed adolescents. Front. Neural Circuits 10, 98.
Lu, H., et al., 2003. Functional magnetic resonance imaging based on changes in vascular space occupancy. Magn. Reson. Med. 50 (2), 263–274.
Luborzewski, A., et al., 2007. Metabolic alterations in the dorsolateral prefrontal cortex after treatment with high-frequency repetitive transcranial magnetic stimulation in patients with unipolar major depression. J. Psychiatr. Res. 41 (7), 606–615.
Maddock, R.J., Buonocore, M.H., 2012. MR spectroscopic studies of the brain in psychiatric disorders. Curr Top Behav Neurosci 11, 199–251.
Maeda, F., et al., 2000. Interindividual variability of the modulatory effects of repetitive transcranial magnetic stimulation on cortical excitability. Exp. Brain Res. 133 (4), 425–430.
Mandal, P.K., 2012. In vivo proton magnetic resonance spectroscopic signal processing for the absolute quantitation of brain metabolites. Eur. J. Radiol. 81 (4), e653–e664.
Mangia, S., et al., 2003. The aerobic brain: lactate decrease at the onset of neural activity. Neuroscience 118 (1), 7–10.
Mangia, S., et al., 2006. Sensitivity of single-voxel 1H-MRS in investigating the metabolism of the activated human visual cortex at 7 T. Magn. Reson. Imaging 24 (4), 343–348.
Mangia, S., et al., 2007. Dynamics of lactate concentration and blood oxygen level-dependent effect in the human visual cortex during repeated identical stimuli. J. Neurosci. Res. 85 (15), 3340–3346.
Marjanska, M., et al., 2013. Brain dynamic neurochemical changes in dystonic patients: a magnetic resonance spectroscopy study. Mov. Disord. 28 (2), 201–209.
Marsman, A., et al., 2013. Glutamate changes in healthy young adulthood. Eur. Neuropsychopharmacol. 23 (11), 1484–1490.
Mathews, V.P., et al., 1995. Cerebral metabolites in patients with acute and subacute strokes: concentrations determined by quantitative proton MR spectroscopy. AJR Am. J. Roentgenol. 165 (3), 633–638.
Maudsley, A.A., Govind, V., Arheart, K.L., 2012. Associations of age, gender and body mass with 1H MR-observed brain metabolites and tissue distributions. NMR Biomed. 25 (4), 580–593.
McDonnell, M.N., Orekhov, Y., Ziemann, U., 2006. The role of GABA(B) receptors in intracortical inhibition in the human motor cortex. Exp. Brain Res. 173 (1), 86–93.
Mescher, M., et al., 1998. Simultaneous *in vivo* spectral editing and water suppression. NMR Biomed. 11 (6), 266–272.
Michael, N., et al., 2003. Metabolic changes after repetitive transcranial magnetic stimulation (rTMS) of the left prefrontal cortex: a sham-controlled proton magnetic resonance spectroscopy (1H MRS) study of healthy brain. Eur. J. Neurosci. 17 (11), 2462–2468.
Michou, E., et al., 2015. fMRI and MRS measures of neuroplasticity in the pharyngeal motor cortex. Neuroimage 117, 1–10.
Mikkelsen, M., et al., 2016. Quantification of gamma-aminobutyric acid (GABA) in (1) H MRS volumes composed heterogeneously of grey and white matter. NMR Biomed. 29 (11), 1644–1655.
Mirza, Y., et al., 2006. Increased medial thalamic creatine-phosphocreatine found by proton magnetic resonance spectroscopy in children with obsessive-compulsive disorder versus major depression and healthy controls. J. Child Neurol. 21 (2), 106–111.
Moffett, J.R., et al., 2007. N-Acetylaspartate in the CNS: from neurodiagnostics to neurobiology. Prog. Neurobiol. 81 (2), 89–131.
Moher, D., et al., 2009. Preferred reporting items for systematic reviews and meta-analyses: the PRISMA statement. PLoS Med. 6 (7), e1000097.
Mooney, R.A., Cirillo, J., Byblow, W.D., 2017. GABA and primary motor cortex inhibition in young and older adults: a multimodal reliability study. J. Neurophysiol. 118 (1), 425–433.
Naressi, A., et al., 2001. Java-based graphical user interface for MRUI, a software package for quantitation of *in vivo*/medical magnetic resonance spectroscopy signals. Comput. Biol. Med. 31 (4), 269–286.
Neale, J.H., Bzdega, T., Wroblewska, B., 2000. N-Acetylaspartylglutamate: the most abundant peptide neurotransmitter in the mammalian central nervous system. J. Neurochem. 75 (2), 443–452.
Ni, Z., et al., 2009. Two phases of interhemispheric inhibition between motor related cortical areas and the primary motor cortex in human. Cereb. Cortex 19 (7), 1654–1665.
Nieminen, J.O., et al., 2019. Short-interval intracortical inhibition in human primary motor cortex: a multi-locus transcranial magnetic stimulation study. Neuroimage 203, 116194.
Opie, G.M., et al., 2017. Investigating TMS-EEG indices of long-interval intracortical inhibition at different interstimulus intervals. Brain Stimul 10 (1), 65–74.
Orth, M., Snijders, A.H., Rothwell, J.C., 2003. The variability of intracortical inhibition and facilitation. Clin. Neurophysiol. 114 (12), 2362–2369.
Oz, G., et al., 2014. Clinical proton MR spectroscopy in central nervous system disorders. Radiology 270 (3), 658–679.

Oz, G., et al., 2020. Advanced single voxel (1) H magnetic resonance spectroscopy techniques in humans: experts' consensus recommendations. NMR Biomed. e4236.
Pascual-Leone, A., et al., 1994. Responses to rapid-rate transcranial magnetic stimulation of the human motor cortex. Brain 117 (Pt 4), 847–858.
Paslakis, G., et al., 2014. N-acetyl-aspartate (NAA) as a correlate of pharmacological treatment in psychiatric disorders: a systematic review. Eur. Neuropsychopharmacol. 24 (10), 1659–1675.
Pogarell, O., et al., 2006. Striatal dopamine release after prefrontal repetitive transcranial magnetic stimulation in major depression: preliminary results of a dynamic [123I] IBZM SPECT study. J. Psychiatr. Res. 40 (4), 307–314.
Pogarell, O., et al., 2007. Acute prefrontal rTMS increases striatal dopamine to a similar degree as D-amphetamine. Psychiatry Res. 156 (3), 251–255.
Pohl, C., et al., 2001. Proton magnetic resonance spectroscopy and transcranial magnetic stimulation for the detection of upper motor neuron degeneration in ALS patients. J. Neurol. Sci. 190 (1–2), 21–27.
Posse, S., et al., 1997. In vivo measurement of regional brain metabolic response to hyperventilation using magnetic resonance: proton echo planar spectroscopic imaging (PEPSI). Magn. Reson. Med. 37 (6), 858–865.
Posse, S., et al., 2013. MR spectroscopic imaging: principles and recent advances. J. Magn. Reson. Imaging 37 (6), 1301–1325.
Pouwels, P.J., Frahm, J., 1998. Regional metabolite concentrations in human brain as determined by quantitative localized proton MRS. Magn. Reson. Med. 39 (1), 53–60.
Premoli, I., et al., 2014a. TMS-EEG signatures of GABAergic neurotransmission in the human cortex. J. Neurosci. 34 (16), 5603–5612.
Premoli, I., et al., 2014b. Characterization of GABAB-receptor mediated neurotransmission in the human cortex by paired-pulse TMS-EEG. Neuroimage 103, 152–162.
Prichard, J., et al., 1991. Lactate rise detected by 1H NMR in human visual cortex during physiologic stimulation. Proc. Natl. Acad. Sci. U. S. A. 88 (13), 5829–5831.
Prinsen, H., et al., 2017. Reproducibility measurement of glutathione, GABA, and glutamate: towards *in vivo* neurochemical profiling of multiple sclerosis with MR spectroscopy at 7T. J. Magn. Reson. Imaging 45 (1), 187–198.
Provencher, S.W., 2001. Automatic quantitation of localized *in vivo* 1H spectra with LCModel. NMR Biomed. 14 (4), 260–264.
Puri, B.K., et al., 1998. The human motor cortex after incomplete spinal cord injury: an investigation using proton magnetic resonance spectroscopy. J. Neurol. Neurosurg. Psychiatry 65 (5), 748–754.
Qiao, J., et al., 2016. The positive effects of high-frequency right dorsolateral prefrontal cortex repetitive transcranial magnetic stimulation on memory, correlated with increases in brain metabolites detected by proton magnetic resonance spectroscopy in recently detoxified alcohol-dependent patients. Neuropsychiatr. Dis. Treat. 12, 2273–2278.
Rae, C.D., 2014. A guide to the metabolic pathways and function of metabolites observed in human brain 1H magnetic resonance spectra. Neurochem. Res. 39 (1), 1–36.
Reyngoudt, H., et al., 2012. Age-related differences in metabolites in the posterior cingulate cortex and hippocampus of normal ageing brain: a 1H-MRS study. Eur. J. Radiol. 81 (3), e223–e231.
Rogasch, N.C., Daskalakis, Z.J., Fitzgerald, P.B., 2013. Mechanisms underlying long-interval cortical inhibition in the human motor cortex: a TMS-EEG study. J. Neurophysiol. 109 (1), 89–98.
Roick, H., von Giesen, H.J., Benecke, R., 1993. On the origin of the postexcitatory inhibition seen after transcranial magnetic brain stimulation in awake human subjects. Exp. Brain Res. 94 (3), 489–498.
Rossini, P.M., et al., 1994. Non-invasive electrical and magnetic stimulation of the brain, spinal cord and roots: basic principles and procedures for routine clinical application. Report of an IFCN committee. Electroencephalogr. Clin. Neurophysiol. 91 (2), 79–92.
Rouw, R., Scholte, H.S., 2010. Neural basis of individual differences in synesthetic experiences. J. Neurosci. 30 (18), 6205–6213.
Sappey-Marinier, D., et al., 1992. Effect of photic stimulation on human visual cortex lactate and phosphates using 1H and 31P magnetic resonance spectroscopy. J. Cereb. Blood Flow Metab. 12 (4), 584–592.
Schaller, B., et al., 2013. Net increase of lactate and glutamate concentration in activated human visual cortex detected with magnetic resonance spectroscopy at 7 tesla. J. Neurosci. Res. 91 (8), 1076–1083.
Schaller, B., et al., 2014. Are glutamate and lactate increases ubiquitous to physiological activation? A (1)H functional MR spectroscopy study during motor activation in human brain at 7Tesla. Neuroimage 93 (Pt 1), 138–145.
Schwenkreis, P., et al., 1999. Influence of the N-methyl-D-aspartate antagonist memantine on human motor cortex excitability. Neurosci. Lett. 270 (3), 137–140.
Siebner, H.R., et al., 1998. Continuous intrathecal baclofen infusions induced a marked increase of the transcranially evoked silent period in a patient with generalized dystonia. Muscle Nerve 21 (9), 1209–1212.
Siebner, H.R., et al., 2019. Distilling the essence of TMS-evoked EEG potentials (TEPs): a call for securing mechanistic specificity and experimental rigor. Brain Stimul. 12 (4), 1051–1054.
Singh, S., et al., 2009. A magnetic resonance spectroscopy study of brain glutamate in a model of plasticity in human pharyngeal motor cortex. Gastroenterology 136 (2), 417–424.
Stagg, C.J., et al., 2009. Neurochemical effects of theta burst stimulation as assessed by magnetic resonance spectroscopy. J. Neurophysiol. 101 (6), 2872–2877.
Stagg, C.J., et al., 2011. Relationship between physiological measures of excitability and levels of glutamate and GABA in the human motor cortex. J. Physiol. 589 (Pt 23), 5845–5855.
Stanley, J.A., Raz, N., 2018. Functional magnetic resonance spectroscopy: the "New" MRS for cognitive neuroscience and psychiatry research. Front Psychiatry 9, 76.
Stefan, K., et al., 2000. Induction of plasticity in the human motor cortex by paired associative stimulation. Brain 123 (Pt 3), 572–584.
Suri, S., et al., 2017. Effect of age and the APOE gene on metabolite concentrations in the posterior cingulate cortex. Neuroimage 152, 509–516.
Tayoshi, S., et al., 2009. Metabolite changes and gender differences in schizophrenia using 3-Tesla proton magnetic resonance spectroscopy (1H-MRS). Schizophr. Res. 108 (1–3), 69–77.
Terhune, D.B., et al., 2011. Enhanced cortical excitability in grapheme-color synesthesia and its modulation. Curr. Biol. 21 (23), 2006–2009.
Terhune, D.B., et al., 2015. Phosphene perception relates to visual cortex glutamate levels and covaries with atypical visuospatial awareness. Cereb. Cortex 25 (11), 4341–4350.
Terpstra, M., et al., 2016. Test-retest reproducibility of neurochemical profiles with short-echo, single-voxel MR spectroscopy at 3T and 7T. Magn. Reson. Med. 76 (4), 1083–1091.
Tkac, I., et al., 2001. In vivo 1H NMR spectroscopy of the human brain at 7 T. Magn. Reson. Med. 46 (3), 451–456.
Tremblay, S., et al., 2013. Relationship between transcranial magnetic stimulation measures of intracortical inhibition and spectroscopy measures of GABA and glutamate+glutamine. J. Neurophysiol. 109 (5), 1343–1349.
Tremblay, S., et al., 2014. Multimodal assessment of primary motor cortex integrity following sport concussion in asymptomatic athletes. Clin. Neurophysiol. 125 (7), 1371–1379.
Udupa, K., Chen, R., 2013. Central motor conduction time. Handb. Clin. Neurol. 116, 375–386.
van Rijen, P.C., et al., 1989. 1H and 31P NMR measurement of cerebral lactate, high-energy phosphate levels, and pH in humans during voluntary hyperventilation: associated EEG, capnographic, and Doppler findings. Magn. Reson. Med. 10 (2), 182–193.
Vidal-Pineiro, D., et al., 2015. Neurochemical modulation in posteromedial default-mode network cortex induced by transcranial magnetic stimulation. Brain Stimul 8 (5), 937–944.
Vidya Shankar, R., et al., 2019. Fast data acquisition techniques in magnetic resonance spectroscopic imaging. NMR Biomed. 32 (3), e4046.
Wallimann, T., et al., 1992. Intracellular compartmentation, structure and function of creatine kinase isoenzymes in tissues with high and fluctuating energy demands: the 'phosphocreatine circuit' for cellular energy homeostasis. Biochem. J. 281 (Pt 1), 21–40.
Walls, A.B., et al., 2015. The glutamine-glutamate/GABA cycle: function, regional differences in glutamate and GABA production and effects of interference with GABA metabolism. Neurochem. Res. 40 (2), 402–409.
Wang, Y., Li, S.J., 1998. Differentiation of metabolic concentrations between gray matter and white matter of human brain by *in vivo* 1H magnetic resonance spectroscopy. Magn. Reson. Med. 39 (1), 28–33.
Wassermann, E.M., 2002. Variation in the response to transcranial magnetic brain stimulation in the general population. Clin. Neurophysiol. 113 (7), 1165–1171.
Werhahn, K.J., et al., 1999. Differential effects on motorcortical inhibition induced by blockade of GABA uptake in humans. J. Physiol. 517 (Pt 2), 591–597.
Wilson, M., et al., 2011. A constrained least-squares approach to the automated quantitation of *in vivo* (1)H magnetic resonance spectroscopy data. Magn. Reson. Med. 65 (1), 1–12.
Wilson, M., et al., 2019. Methodological consensus on clinical proton MRS of the brain: review and recommendations. Magn. Reson. Med. 82 (2), 527–550.
Wolters, A., et al., 2003. A temporally asymmetric Hebbian rule governing plasticity in the human motor cortex. J. Neurophysiol. 89 (5), 2339–2345.
Zeller, D., et al., 2010. Rapid-onset central motor plasticity in multiple sclerosis. Neurology 74 (9), 728–735.
Zeller, D., et al., 2011. Functional role of ipsilateral motor areas in multiple sclerosis. J. Neurol. Neurosurg. Psychiatry 82 (5), 578–583.
Zhai, P., et al., 2003. Primary lateral sclerosis: a heterogeneous disorder composed of different subtypes? Neurology 60 (8), 1258–1265.
Zhang, F., et al., 2019. High-frequency repetitive transcranial magnetic stimulation combined with cognitive training improves cognitive function and cortical metabolic ratios in Alzheimer's disease. J. Neural Transm. 126 (8), 1081–1094.
Zheng, H., et al., 2010. High-frequency rTMS treatment increases left prefrontal myo-inositol in young patients with treatment-resistant depression. Prog. Neuropsychopharmacol. Biol. Psychiatry 34 (7), 1189–1195.
Zheng, H., et al., 2015. Abnormal anterior cingulate N-acetylaspartate and executive functioning in treatment-resistant depression After rTMS therapy. Int. J. Neuropsychopharmacol. 18 (11), pyv059.
Zhu, X.H., Chen, W., 2001. Observed BOLD effects on cerebral metabolite resonances in human visual cortex during visual stimulation: a functional (1)H MRS study at 4 T. Magn. Reson. Med. 46 (5), 841–847.
Ziemann, U., Lonnecker, S., Paulus, W., 1995. Inhibition of human motor cortex by ethanol. A transcranial magnetic stimulation study. Brain 118 (Pt 6), 1437–1446.
Ziemann, U., et al., 1996. The effect of lorazepam on the motor cortical excitability in man. Exp. Brain Res. 109 (1), 127–135.
Ziemann, U., et al., 1998. Dextromethorphan decreases the excitability of the human motor cortex. Neurology 51 (5), 1320–1324.
Ziemann, U., et al., 2015. TMS and drugs revisited 2014. Clin. Neurophysiol. 126 (10), 1847–1868.
Ziemann, U., Romani, G.L., Ilmoniemi, R.J., 2019. ["ConnectToBrain": synergy project for therapeutic closed-loop stimulation of brain network disorders]. Nervenarzt 90 (8), 804–808.